scientific reports

Check for updates

OPEN

Experimental investigation of divalent ions and CTAB effects on heavy oil emulsion stability in carbonate reservoirs

Alireza Tajik Mansouri, Mina Sadat Mahdavi & Amir Hossein Saeedi Dehaghani✉

Low-salinity water injection can boost oil extraction but often triggers asphaltene instability, leading to damaging emulsions and clogging in carbonate reservoirs. This research explores a solution by combining ion-tuned brines with a cationic surfactant (cetyltrimethylammonium bromide (CTAB)) to manage these effects. We specifically examine how the ionic composition of injected water, when mixed with CTAB and reservoir rock particles (calcite), governs emulsion behavior and oil recovery potential. A series of laboratory experiments simulated reservoir conditions by mixing heavy crude oil with various brines and calcite particles. Key experimental evaluations were performed, including measurements of interfacial tension (IFT), emulsion fraction and separation time, changes in rock surface wettability, and analyses by Fourier-transform infrared (FTIR) spectroscopy, zeta potential, and SARA (Saturates, Aromatics, Resins, and Asphaltenes). The result showed that brines enriched with sulfate ions, in combination with CTAB, resulted in the most favorable outcome. This system reduced the interfacial tension to 5.5 mN/m, whereas the magnesium-modified seawater in the presence of CTAB achieved only about 20 mN/m. Furthermore, the sulfate–CTAB mixture altered the calcite surface toward a more water-wet condition, a change that plays a critical role in enhancing the displacement of trapped oil. The emulsion analysis showed that using sulfate-enriched seawater in the presence of calcite particles and CTAB reduced asphaltene precipitation and produced less stable emulsions that break more easily. This helps lower the chance of formation damage. In contrast, brines high in magnesium or calcium cations promoted the formation of rigid asphaltene complexes that stabilized emulsions and hindered oil mobilization. SARA and zeta potential results showed that in the aged oil–(SW10d.4SO_4) system (the oil was exposed to sulfate-enriched seawater in the presence of CTAB and calcite), the less-negatively charged oil components tended to migrate. In contrast, cation-rich brines interacted more strongly with the negatively charged asphaltenes, removing them preferentially over the less-polar components and resin fractions. The FTIR-derived indices clearly indicated that different brine compositions in the presence of CTAB and calcite particles influenced the contribution of various oil components to the fluid–fluid interfacial interactions. The long chain index (LCI), representing less-polar hydrocarbon groups, showed the lowest value in aged oil–(SW10d.4SO_4), consistent with the migration of these fractions. Meanwhile, in the aged oil–(SW10d.4Mg) system (oil exposed to magnesium-enriched seawater with CTAB and calcite), the polar aromatic (PA) index and the aliphatic index (ALI) reached 0.366 and 0.193, respectively. This indicates the preferential migration and removal of more polar functional groups under cation-rich conditions. Tailoring the injected water with sulfate and surfactant gives two benefits. It improves oil recovery by changing rock–fluid interactions and it keeps operations efficient by reducing problematic emulsion formation.

Keywords Asphaltene molecular structure, Emulsion, Smart water flooding, Heavy oil, Wettability alteration, Zeta potential

Water flooding is one of the most widely implemented oil recovery strategies, applied in heavy oil reservoirs to maintain reservoir pressure and displace crude oil toward production wells[1]. Recently, significant research efforts have focused on changing the brine composition, such as sulfate (SO_4^{2-}), calcium (Ca^{2+}), and magnesium

Department of Petroleum Engineering, Faculty of Chemical Engineering, Tarbiat Modares University, Tehran, Iran. ✉email: asaeedi@modares.ac.ir

(Mg^{2+}), in the injected aqueous phase —a technique commonly referred to as low-salinity water or ion-tuned water or smart water flooding—to improve oil displacement efficiency and reservoir performance[2–4]. This approach has revealed strong potential for improving the recovery of heavy crude oil, particularly in carbonate formations, by changing wettability and the interfacial properties between oil and water phases[5,6]. However, the precise mechanisms responsible for these improvements are not yet fully understood.

Despite its advantages, ion-tuned water flooding can also produce unintended challenges, such as increased emulsion formation and asphaltene destabilization, effects that are especially pronounced in carbonate reservoirs[7,8]. The formation of emulsions poses a significant challenge in enhanced oil recovery (EOR), as it can reduce production efficiency and contribute to both economic losses and environmental concerns. Emulsification increases the apparent viscosity of crude oil, making fluid handling and transportation more difficult while complicating oil–water separation processes at production facilities[8,9]. This issue often leads to serious operational complications, including pipeline blockages, increased processing demands, and a decline in overall crude oil quality[8,10,11]. Therefore, there is a need to design effective strategies that mitigate emulsion stability and promote production performance in carbonate reservoirs subjected to low-salinity water flooding.

One of the key challenges is the enhanced emulsion formation resulting from complex interactions between the injected brine, calcite particles, and heavy oil fractions[5]. Calcite particles can aid in the adsorption of polar components of heavy oil, like asphaltene and resin particles. Thus, this can facilitate the development of stable Pickering emulsions. These emulsions are stabilized by solid particles at the oil–brine interface[12,13].

Emulsion formation and stability are largely governed by asphaltene molecules, which accumulate at the oil–water interface and reinforce interfacial films[14,15]. Asphaltenes are high-molecular-weight components of crude oil with intricate polyaromatic groups and a diverse functional groups, ranging from highly polar to weakly polar. This unique combination enables them to preferentially adsorb at oil–water interfaces, where they reduce interfacial tension and form rigid interfacial films. This interfacial layer reinforces emulsion stability by mechanically hindering droplet coalescence and maintaining the integrity of water-in-oil dispersions over extended periods[5,16].

Tajikmansori et al. demonstrated that the unique structural features and electrostatic characteristics of asphaltene molecules play a pivotal role in governing interfacial interactions, directly affecting the stability, organization, and mechanical strength of the crude oil–water interface[2,17]. Additionally, Liang et al. demonstrated that the asphaltenes concentration in heavy oil, as well as nitrogen-, sulfur-, and oxygen-containing (NSO) compounds, significantly influence the physicochemical properties of the oil–water interface, including interfacial tension, film rigidity, and emulsion stability[18]. Joonaki et al. showed that in aqueous environments with higher salinity, asphaltenes tend to form larger polyaromatic aggregates, which can significantly alter interfacial structure and contribute to enhanced emulsion stability[19]. Therefore, understanding the influence of oil constituents, particularly asphaltenes and resins, on emulsion behavior is essential for elucidating mechanisms that govern emulsion formation and stability.

Numerous studies have also investigated the effects of low salinity water and solid particles on emulsion properties. For instance, Balavi et al. examined the combined influence of ionic composition and calcite minerals on both emulsion stability and asphaltene behavior. Their findings indicated that in high-salinity water, asphaltenes exhibited enhanced tendency to the interaction on rock surface, which in turn altered the stability and characteristics of the resulting emulsions[5]. In a separate study, Cai et al. clarified that particles, which act as stabilizers and improve emulsions, can also reduce interfacial tension[20].

Mahdavi et al. further highlighted the role of solid particles, finding that the combination of clay, high-salinity brine, and asphaltene and resin molecules synergistically created emulsions of exceptional stability[10,15]. In addition, Zhou et al. demonstrated that the synergistic effect of kaolinite and active ions can significantly alter emulsion stability. This finding contributed to a better understanding of mechanisms relevant to heavy oil extraction[21].

Cationic surfactants, such as CTAB, have been investigated in EOR performance due to their multiple functional roles. CTAB is effective in altering the wettability of reservoir rocks toward a more water-wet state, thereby promoting the displacement of residual hydrocarbons. In addition, it substantially lowers the interfacial tension (IFT) between oil and water, facilitating the mobilization of trapped oil. Depending on the specific reservoir conditions and fluid compositions, CTAB can either stabilize or destabilize emulsions, highlighting its contribution as a chemical agent for improving oil recovery efficiency[22–24]. The amphiphilic nature of CTAB, consisting of a positively charged headgroup and a hydrophobic tail, allows it to interact simultaneously with both polar and nonpolar components in the reservoir. These interactions modify the interfacial film and can change emulsion stability, depending on the composition of the oil and brine phases[2,25,26].

The influence of CTAB on oil-water interface and emulsion characteristics, including its stability, has been extensively investigated in a wide range of studies, highlighting its critical role in modulating interfacial properties and controlling droplet behavior[27–29]. For example, Seng et al. explored the interactions between heavy oil and surfactants, revealing that saturated hydrocarbon fractions promote the formation of stable emulsions[22]. In a related investigation, Koreh et al. analyzed how different surfactants affect the properties of the fluid–fluid interface. Their findings demonstrated that surfactant selection plays a pivotal role in controlling both the initial formation of emulsions and their subsequent stability over time[30].

Furthermore, Javadi et al. demonstrated that the adsorption of CTAB at the oil-water interface, where hydrophobic tails extend into the oil phase, was highly dependent on both surfactant concentration and brine ionic strength[31]. Zallaghi et al. demonstrated that the injection of surfactant and smart water enhanced oil recovery, underscoring the effectiveness of this strategy in improving overall EOR performance[32].

The accumulation of surfactant in carbonate reservoirs during low-salinity water flooding is strongly influenced by both the brine's ionic composition and the rock mineralogy. Research by Rezavni et al. demonstrated that a synergistic interaction between surfactants and solid particles significantly enhance oil recovery, even

when employed at low concentrations[33]. Also, experimental evidence from Liu et al. confirmed that the ionic composition of the brine, specifically the presence of $CaCl_2$, was a major factor governing the extent of surfactant adsorption onto solid particles such as clay[34].

Divandari et al. investigated the synergistic effects of ion-tuned seawater, nanoparticles, and surfactants, finding that their combination markedly altered interfacial tension[35]. The critical role of surfactant charge was underscored by Li et al. They showed that ionic surfactants like CTAB markedly influence interfacial behavior in complex systems containing nanoparticles and ions, unlike their non-ionic counterparts[36]. Therefore, a detailed study of the interactions between CTAB, oil components, ions, and calcite, both in the emulsion phase and at the rock–fluid interface, is essential. This understanding is necessary to devise targeted solutions for the persistent problems caused by heavy oil emulsions.

To address the critical challenge of emulsion stability in low-salinity water flooding and improve heavy oil recovery, this work introduces a targeted chemical method that utilizes the synergistic interplay between specific brine ions, calcite particles, asphaltene molecules, and a cationic surfactant. We present a comprehensive experimental investigation into how calcium, magnesium, and sulfate ions, in conjunction with CTAB, the polar components of oil, and reservoir calcite particles, influence the complex interplay at the oil-water-rock interface. In this regard, a new experimental protocol was developed to investigate the synergistic effects of oil components, calcite, CTAB molecules, and brine salinity. First, emulsion samples were prepared and aged at reservoir-relevant temperature for 20 days. After preparing the emulsions, they were separated, and the fluid-fluid, rock-fluid, and oil phases were analyzed using a set of experimental tests. The fluid–fluid and oil phases were characterized using interfacial tension, zeta potential, SARA, and FTIR analyses. Additionally, the rock–fluid interactions were evaluated by measuring the zeta potential to find the surface charge and the contact angle on calcite to see how the wettability changed. By comparing emulsion stability, interfacial tension, zeta potential, and wettability results with FTIR and SARA data, we show that the simultaneous use of CTAB and smart water can reduce harmful asphaltene precipitation and improve emulsion behavior.

Materials and methods

Materials

Oil sample

The crude oil used in this study was sourced from a field in southern Iran, and its composition and properties are summarized in Table 1. As shown in Table 1, the viscosity of the crude oil is 426.3 cP. According to previous studies, oils with viscosities in this range are classified as heavy crude oils[10,15].

Water phase

This research focused on examining the combined effects of calcite particles, the cationic surfactant cetyltrimethylammonium bromide (CTAB), and low-salinity water. Persian Gulf seawater served as the base fluid for smart water preparation. To evaluate the effect of salinity, the concentrations of the active ions (Mg^{2+}, Ca^{2+}, and SO_4^{2-}) were increased to two and four times their natural concentration. Brine formulations included seawater (SW), seawater diluted tenfold (SW10d), and ion-rich seawater samples, all of which were mixed with CTAB. The surfactant and salts were supplied by Merck (Germany) at >99% purity. Table 2 summarized the composition of the brines used. Both CTAB and calcite particle concentrations were kept constant across all tests, making total dissolved solids (TDS) the only indicator of salinity variation.

$$I = \frac{1}{2}\sum_{i=1}^{n} c_i z_i^2 \tag{1}$$

In this context, c_i' represents the concentration of ion 'i', measured in mol/L, but z_i denotes its corresponding ionic charge[10].

Crude oil Properties (unit)	Result
Density@25°C (g/cm^3)	0.88
Viscosity (cP)	426.3
Acid number (mg KOH/g oil)	0.75
Asphaltene (%mass)	14.35
Resin (%mass)	15.20
Saturates	33.30
Aromatic	37.15

Table 1. Basic properties and SARA (Saturates, Aromatics, Resins, Asphaltenes) analysis of the heavy crude oil sample used in the study[10].

No.	Solutions	NaCl (g/L)	Na_2SO_4 (g/L)	$CaCl_2$ (g/L)	$MgCl_2.6H_2O$ (g/L)	KCl (g/L)	Calcite (g/L)	CTAB (g/L)	Ionic Strength(I)	TDS (ppm)
1	SW	28.323	4.936	1.630	10.520	1.032	1	0.386	0.802	46,431
2	SW10d	5.664	0.987	0.326	2.104	0.206	1	0.386	0.160	9,287
3	SW10d.2Ca	5.664	0.987	3.260	2.104	0.206	1	0.386	0.240	12,221
4	SW10d.4Ca	5.664	0.987	6.520	2.104	0.206	1	0.386	0.328	15,481
5	SW10d.2Mg	5.664	0.987	0.326	21.040	0.206	1	0.386	0.440	28,223
6	SW10d.4Mg	5.664	0.987	0.326	42.080	0.206	1	0.386	0.750	49.263
7	SW10d.2SO4	5.664	9.872	0.326	2.104	0.206	1	0.386	0.348	18,172
8	SW10d.4SO4	5.664	19.744	0.326	2.104	0.206	1	0.386	0.556	28,044

Table 2. Detailed ionic composition, TDS, and ionic strength of the Brine solutions prepared for the experiments[15].

Compositions	Result(%mass)	Compositions	Result(%mass)
CaO	54.890	SO_3	0.867
MgO	0.465	Zn	0.098
P_2O_5	0.076	Fe_2O_3	0.291
Al_2O_3	0.250	SiO_2	0.731
Cl	0.017	Sr	0.260
K_2O	0.09	Loss in ignition (LOI)	41.965

Table 3. Chemical composition of the purified calcite particles by X-ray fluorescence analysis[2].

Calcite particles

Calcite particles were utilized in this study to evaluate the synergistic interactions among carbonate minerals, injected ions, CTAB, and heavy components of crude oil. Their mineral composition was determined through X-ray fluorescence (XRF) analysis, with the results given in Table 3.

Method

Sample preparation

To investigate emulsion stability, mixtures of crude oil, brine solutions, CTAB, and calcite particles were prepared in 100 mL glass bottles with a water-to-oil ratio of 60:40 (v/v)[10,37]. Brine samples were pre-mixed with CTAB and calcite particles before adding crude oil. An ultrasonic probe was used to disperse the oil phase uniformly into the aqueous phase, ensuring thorough mixing of all components.

The emulsified mixtures were further homogenized using a magnetic stirrer operating at 1000 rpm for 6 h at 25 °C. After homogenization, the samples were placed in a convection oven at 80 °C and aged for 20 days. It is worth mentioning that a temperature of 80 °C was selected for the thermal aging experiments to closely reflect the conditions of the heavy oil reservoirs examined in this study[10,37]. This thermal aging period allowed sufficient time for essential physicochemical processes, such as cation exchange, asphaltene interaction with mineral surfaces, and reorganization of the interfacial film[38].

Once aged, samples were centrifuged at 4000 rpm in 5-minute intervals until clear separation of oil, water, and solids was observed. Separated emulsions were then stored at 25 °C in a dark chamber for 24 h to stabilize the separated phases before analysis. The emulsion eventually separated into three distinct phases: oil, water, and solids. It is important to mention that the solid phase mainly consisted of calcite particles with adsorbed asphaltenes, as well as aggregates of unstable asphaltenes that precipitated during the aging process. The volumes of the solid and oil phases were measured to evaluate the overall stability of the emulsion[39].

For further testing, oil samples were carefully collected from the upper layer of the centrifuged bottles. To ensure complete removal of residual water droplets and calcite particles, the extracted oil underwent two additional centrifugation cycles. The resulting purified sample was referred to as the "aged oil–aqueous phase". All experiments were performed in triplicate to verify repeatability and accuracy.

IFT (interfacial tension) measurement

Interfacial tension (IFT) measurements were performed to gain deeper insight into the fluid–fluid interfacial phenomena. To analyze fluid–fluid interfacial behavior, the interfacial tension (IFT) between the oil sample and various brine solutions was measured using the pendant drop technique[15,40]. In this method, a droplet of crude oil is carefully dispensed via a needle into a cell containing the brine with CTAB. For high-viscosity oil, the needle tip was placed just below the surface of the aqueous phase, and the oil was injected slowly at a controlled rate to avoid distorting the droplet. The pendant-drop method is ideal for heavy oils because it enables the droplet to form under carefully controlled pressure[41,42]. This ensures stable formation and accurate interfacial tension measurements. Once the oil–water interface reaches equilibrium, the interfacial tension (IFT)

was calculated by analyzing droplet pictures with specialized image-processing software. The schematic of the interfacial tension (IFT) measurement is shown in Fig. 1.

Zeta (ζ) potential measurement

The ζ potential of calcite particles was measured under standardized laboratory conditions at 25 °C and atmospheric pressure (14.7 psi). All measurements were conducted at a controlled neutral pH of 7 to ensure consistency. Electrophoretic mobility was determined using a MICROTAC particle analyzer, and these data were subsequently converted to zeta potential values.

To prepare samples, a 5 wt% suspension was formulated by dispersing 5 g of finely ground calcite in 100 mL of the selected brine solutions and aged oil in distilled water. The suspensions were first treated with the ultrasonic probe to achieve particle dispersion, followed by mixing on a magnetic stirrer. The pH of each suspension was carefully adjusted to neutrality using either 1 M NaOH or 0.1 M HCl, depending on the initial pH of the brine[10,43]. Each experiment was performed in four replicates, and the average ζ potential values are reported to ensure data reliability.

Fourier transform infrared spectroscopy (FTIR)

FTIR spectroscopy was performed to identify the chemical functionalities present in aged oil recovered from emulsion samples, providing insight into the role of oil components in emulsion stability[44,45]. The spectra were acquired using a PerkinElmer Frontier spectrometer operated in transmission mode, scanning over a wavelength range of 400–4000 cm^{-1}. Prior to analysis, droplets of the aged oil were deposited onto potassium bromide (KBr) pellets to create thin films for examination[15,46,47]. This technique, known for its sensitivity to molecular vibrations and chemical environments, enabled precise characterization of functional groups within the oil phase.

Contact angle measurement

Contact angle measurements were conducted to evaluate wettability alterations of calcite surfaces exposed to brine solutions containing CTAB. High-purity calcite powder was first oven-dried at 80 °C for 24 h to remove residual moisture, then fully hydrated in deionized water for 48 h to stabilize its surface chemistry[40]. To simulate reservoir oil–rock interactions, the hydrated calcite particles were mixed with the oil sample at a 1:10 (g: mL) ratio and aged at 80 °C for 7 days, allowing adsorption of polar oil components[2,48,49].

After aging, unabsorbed oil was removed using filter paper, and the calcite particles were washed with deionized water to remove unabsorbed and loosely bound oil from their surfaces. The treated mineral samples were subsequently immersed in mixed CTAB–brine solutions prepared at concentrations near the surfactant's critical micelle concentration (~0.4 g/L). A solid-to-liquid ratio of 1:10 was used to ensure complete exposure of the mineral surface to the aqueous phase. Samples were kept in sealed containers at 80 °C for the duration of testing.

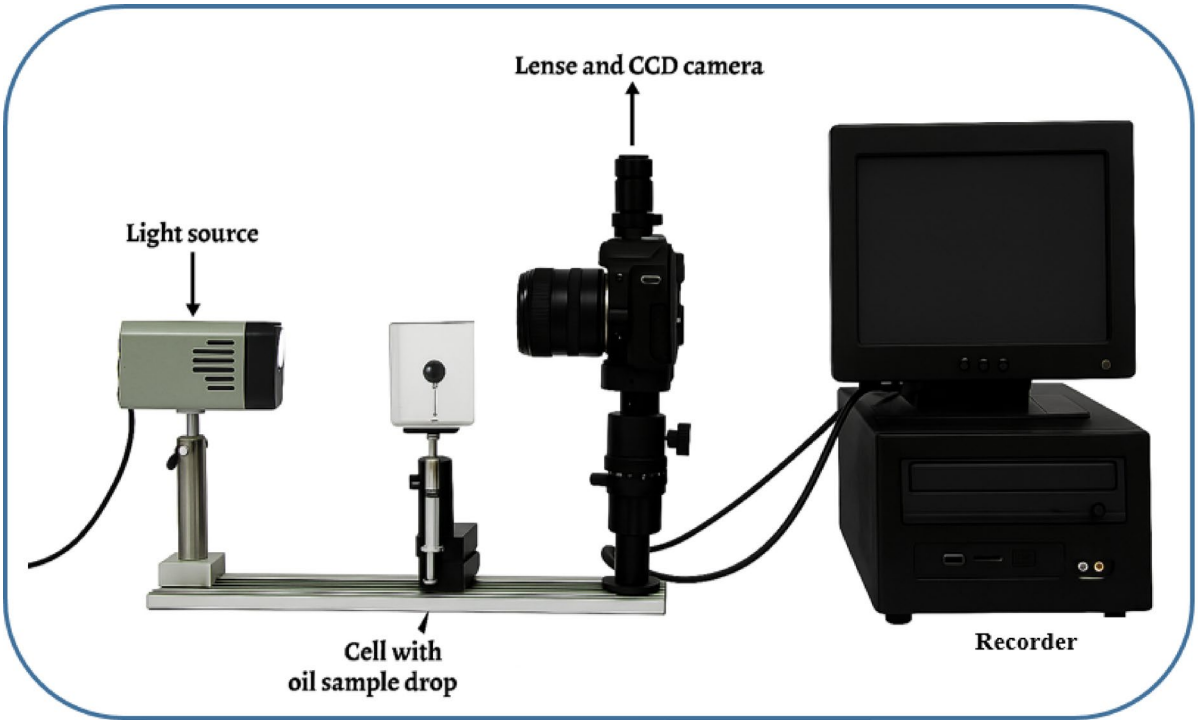

Fig. 1. Schematic diagram of the experimental setup used for interfacial tension (IFT) measurements via the pendant drop method.

For contact angle evaluation, roughly 1 g of calcite powder was extracted from the brine–surfactant mixtures at each testing interval, rinsed, air-dried, and pressed into uniform pellets (2 cm diameter) at 200 kPa·cm^{-2}[40,50,51]. To maintain the natural wettability of calcite, no external binding agents were introduced during pellet formation. Contact angle measurements were conducted at ambient laboratory conditions (~ 25 °C) using a sessile drop goniometer equipped with a temperature-controlled chamber and a macro lens for high-resolution imaging. Observations were taken at predetermined intervals (initially, and at 7, 14, 21, 28, 35, 42, and 49 days), and testing was concluded when the variation between consecutive measurements was below 2°, indicating equilibrium[2,23,40].

SARA analysis

The chemical composition of the crude oil was characterized through SARA (Saturates, Aromatics, Resins, and Asphaltenes) fractionation using established standardized techniques. To quantify these four primary hydrocarbon classes in aged oil samples, liquid chromatography was employed following ASTM D4124 guidelines[52]. This method separates saturates, aromatics, and resins through stepwise elution with solvents of increasing polarity, allowing precise differentiation of each fraction. Asphaltenes, recognized as the most polar and complex fraction, were isolated independently by inducing precipitation with n-heptane as a precipitant, in line with ASTM D6560-17 protocols[15]. This comprehensive analysis provided critical insights into the chemical makeup of the oil and its role in emulsion stability.

Result and discussion

Crude oil contains various heavy molecular components, with asphaltenes being particularly known for accumulating at the oil-water interface. When they are migrated toward the emulsion phase, these molecules produce a dense, elastic layer around water droplets, making it difficult for the droplets to coalesce. This interfacial behavior is one of the key factors behind the stability of emulsions[11,48]. In carbonate reservoirs, where calcite particles are naturally abundant, low-salinity water injection frequently intensifies this effect, causing the formation of emulsions. Such emulsions present significant challenges in petroleum production because they interfere with separation processes and place additional strain on surface handling facilities.

The present work explores a combined chemical approach involving low-salinity water and the surfactant such as CTAB to address these issues. To verify these findings, we designed a comprehensive experimental method. Tests were performed to evaluate the characteristics of the emulsions, the efficiency of oil displacement, interactions between fluids, the influence of heavy oil constituents, and fluid–rock dynamics. Detailed outcomes and their implications are discussed in the subsequent sections.

Emulsion analysis

Mobilizing residual oil left behind after low salinity water flooding can be achieved through emulsification, primarily by reducing the interfacial tension (IFT) between the oil and injected water[53]. This reduction in interfacial tension (IFT) enhances displacement efficiency and facilitates the movement of previously trapped crude oil, making it a key mechanism in many enhanced oil recovery (EOR) strategies[53,54]. The combined action of calcite particles, cationic surfactant of CTAB, and dissolved ions in injected water plays an important role in altering emulsion characteristics and interfacial behavior[55]. In this study, we investigated the stability of emulsions to better understand their behavior under reservoir-like conditions. Emulsion stability was quantified by measuring the proportion of separated emulsions' fractions after centrifugation, as well as by monitoring the time required for phase separation to occur. The corresponding data and analysis are illustrated in Figs. 2 and 3.

Figure 2. shows that the emulsions separated into their fractions, including oil, water, and solid, within a time range of 28 to 70 min. Among the tested brines, magnesium-enriched seawater (SW10d.4Mg) produced the fastest separation, whereas sulfate-rich seawater (SW10d.4SO_4) exhibited the slowest. Similarly, the data in Fig. 3. indicates that adding divalent cations (Mg^{2+}, Ca^{2+}) and sulfate ions (SO_4^{2-}) to seawater noticeably influenced the proportions of oil and solids released from the emulsions. The highest fraction of solids and oil was obtained with emulsion-(SW10d.4Mg) and emulsion-(SW10d.4SO_4), respectively.

In emulsions prepared with seawater containing divalent ions and CTAB, several mechanisms likely govern the interactions among asphaltenes, ionic species, CTAB molecules, and calcite particles. These interactions are discussed below in detail.

1) The ionic composition of smart water plays a decisive role in controlling the structure of the electrical double layer (EDL) at the oil–water interface[56]. Multivalent ions such as magnesium (Mg^{2+}), calcium (Ca^{2+}), and sulfate (SO_4^{2-}) are especially influential because their higher charge density enables them to strongly compress or expand the EDL, depending on their concentration and ionic strength[10,57]. Variations in the EDL thickness directly affect the interfacial environment, influencing how easily surfactant molecules such as CTAB can approach and adsorb at the interface[2,5,58].

2) Divalent cations such as calcium (Ca^{2+}) and magnesium (Mg^{2+}) strongly influence interfacial chemistry by forming complexes with polar molecules in crude oil, particularly asphaltene compounds[59,60]. At the oil–water interface, these interactions lead to the formation of asphaltene–ion complexes, which strengthen the interfacial film. This process is referred to as the complexation mechanism.

The mechanism begins with the dissociation of acidic functional groups present in asphaltene molecules within the oil phase. Carboxylic acid groups (-COOH), for example, deprotonate to produce negatively charged carboxylate ions ($-COO^-$). These anionic sites then attract divalent cations from the aqueous phase, forming asphaltene-ion complexes at the interface[60]. This interaction acts as a molecular bridge that links oil-phase species with water-phase ions. The following equations demonstrate the interaction between the polar component of oil and ions:

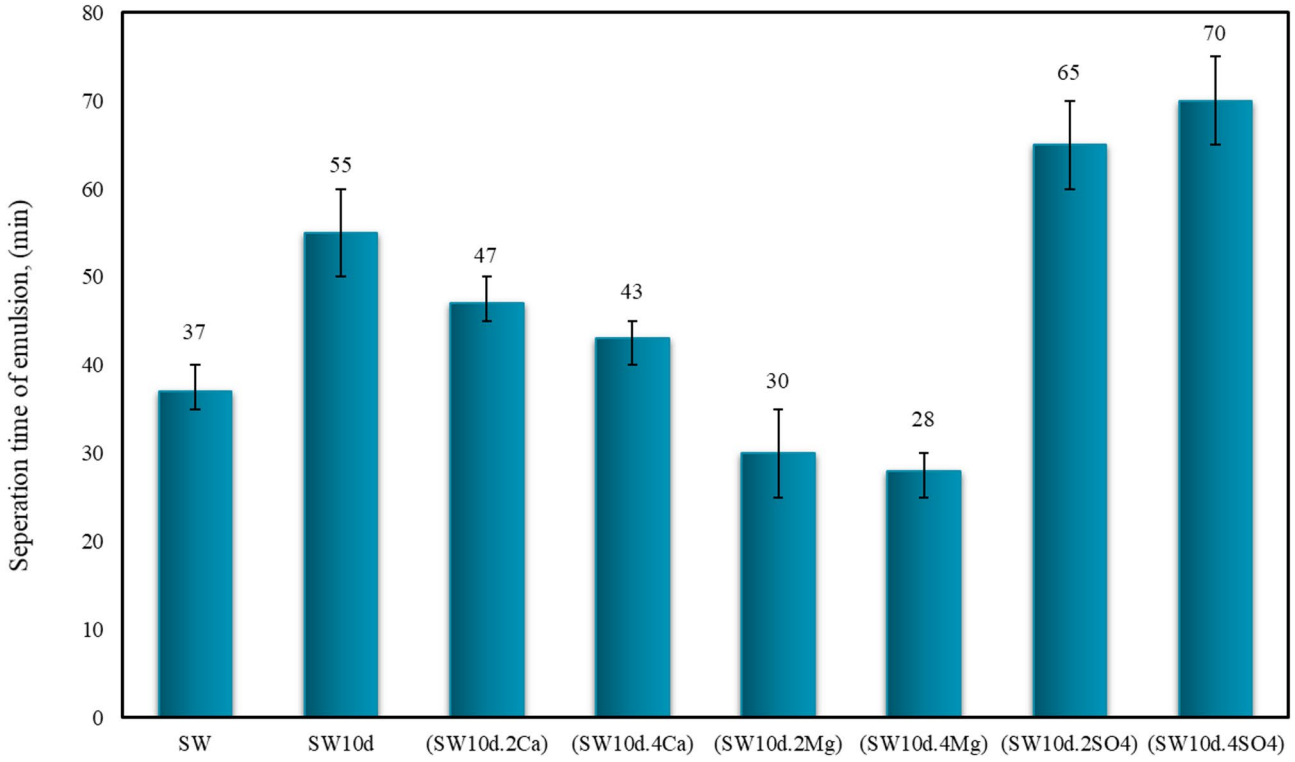

Fig. 2. Emulsion stability assessment by the phase separation time for different ion-tuned brines mixed with CTAB and calcite.

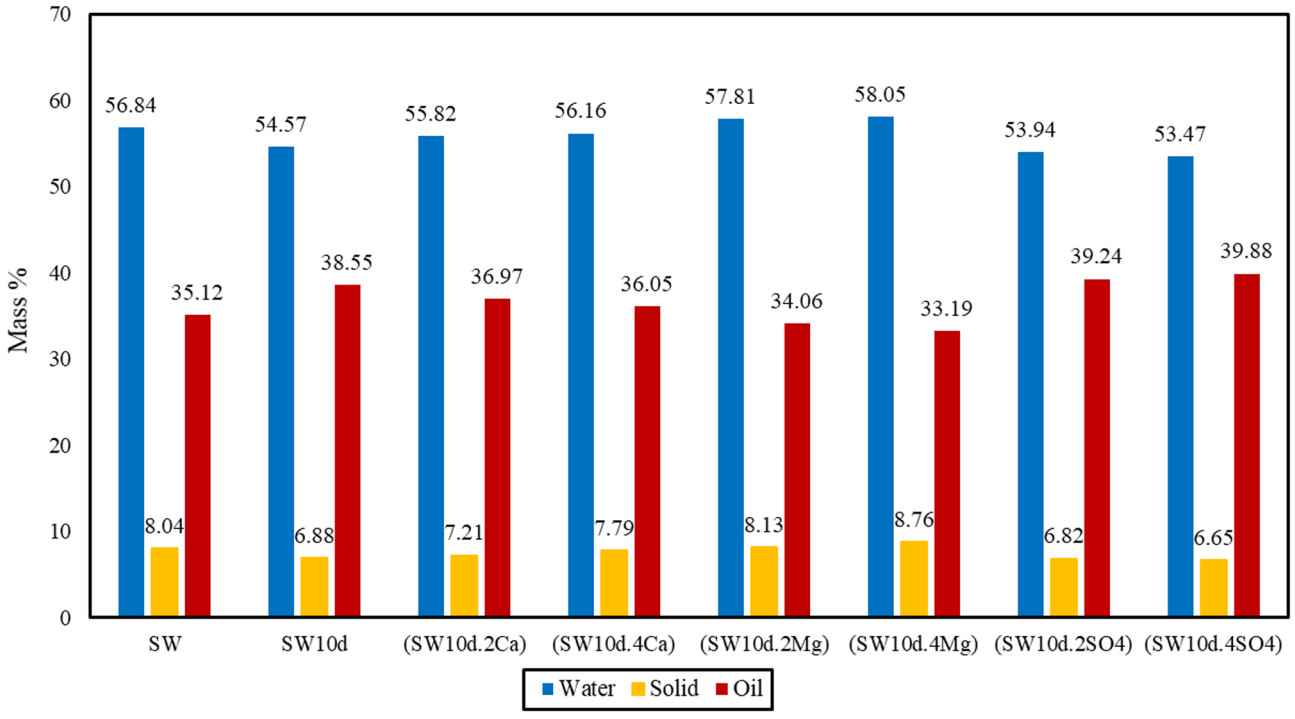

Fig. 3. Distribution of oil, water, and solid fractions in the separated emulsion phase for various brine compositions.

$$\equiv COOH + Ca^{2+} \leftrightarrow \equiv COO - Ca^{+} + H^{+} \quad (2)$$

$$\equiv COOH + Mg^{2+} \leftrightarrow \equiv COO - Mg^{+} + H^{+} \quad (3)$$

3) The salting-in and salting-out phenomena describe how variations in brine salinity influence the interfacial behavior of polar crude oil constituents such as asphaltenes and resins[10,61]. When the concentration of dissolved salts in brine increases, ions like Mg^{2+}, Ca^{2+}, and SO_4^{2-} become heavily hydrated, reducing their presence near the oil–water interface. This ion hydration effect, known as salting-out, limits electrostatic interactions at the interface and decreases the tendency of polar hydrocarbons to adsorb on water droplets, thereby reducing their accumulation at the interfacial film. Nonetheless, decreasing the salinity weakens ion hydration, increasing ionic activity at the interface and promoting the adsorption of polar components, which improves emulsion stability.

The distribution of oil and solid components within the emulsion phases differed significantly between the SW and SW10d samples. As shown in Figs. 2 and 3, the emulsion formed with SW in the presence of CTAB and calcite particles contained a higher proportion of solid particles (8.04%). In contrast, the emulsion formed with diluted seawater (SW10d) contained a greater amount of oil (38.55%).

This difference is attributed to the brine's ionic composition. In the emulsion-SW sample, the high concentration of active cations (e.g., Mg^{2+}, Ca^{2+}) promotes complexation with polar oil components, such as asphaltenes and resins. This complexation, following the mechanisms described in Eqs. 2 and 3, likely increased their migration to the emulsion phase and subsequent formation of solid asphaltene-ion or resin-ion complexes. Furthermore, the abundance of divalent cations competed with the cationic surfactant CTAB for interface occupancy[25,37,62]. This competition enabled more calcite particles to interact with the polar and negatively charged oil molecules, stabilizing the emulsion-SW and contributing to the higher solid content.

On the other hand, the SW10d contained a lower concentration of these active cations. With reduced ionic competition and enough space in the EDL, CTAB more effectively accumulated at the oil-water interface. The high surface activity of CTAB likely limited the migration of polar crude oil components to the interface. Consequently, less asphaltenic solid was formed, and a larger volume of the oil phase itself was incorporated into the emulsion.

This observation was supported by emulsion stability tests. As seen in Fig. 2, the emulsion-SW10d required a longer time to separate than the emulsion-SW, indicating higher stability. The improved emulsion stability, combined with greater oil entrapment, suggests that SW10d enhances the recovery of trapped oil in EOR applications while minimizing solid formation[53].

The stability of the produced emulsions, as directly measured by their phase separation time in Fig. 2, is fundamentally governed by the type and concentration of divalent cations in the brine. The difference in emulsion stability between calcium-rich brines (SW10d.2Ca: 47 min, SW10d.4Ca: 43 min) and magnesium-rich brines (SW10d.2Mg and SW10d.4Mg) highlights two opposing interfacial effects. Calcium-enriched seawater with CTAB and calcite stabilizes the emulsion film, while magnesium-enriched seawater tends to reduce the formation of a stable emulsion.

The greater stability of emulsions with calcium ions, CTAB, and calcite particles appears to arise from synergistic effects at the oil–water interface. Calcium's relatively lower charge density weakens its competitive presence against the cationic surfactant CTAB for accumulation at the interface. This allowed CTAB molecules to maintain a dominant presence at the interface, creating a stable film characterized by strong electrostatic repulsion between cationic head groups in the electrical double layer. Furthermore, the lower calcium concentration in (SW10d.2Ca) promotes a salting-in effect, helping CTAB migrate to the interface more effectively than in (SW10d.4Ca). In (SW10d.4Ca), stronger interactions between Ca^{2+} and asphaltenes lead to the formation of asphaltene–ion or resin–ion complexes, which limit the stability of the CTAB-stabilized emulsion film[17,58,63]. However, the lower concentration of active cations in (SW10d.2Ca) enhances the migration of CTAB molecules to the interface. This increases emulsion stability, strengthens the film, and helps prevent droplet coalescence[38].

Conversely, magnesium ions act as a potent destabilizing agent. Due to their high charge density, Mg^{2+} ions exhibit a strong preferential binding affinity for the negatively charged functional groups in asphaltene and resin molecules. This interaction did not promote a structured film; instead, it directly increases the solid content of the system, as confirmed by the higher percentage of solids in (SW10d.4Mg) compared to (SW10d.4Ca). More importantly, these aggregates effectively compete for and displace CTAB molecules from the interface. The expulsion of the highly surface-active CTAB cripples its ability to stabilize droplets, leading to lower migration of oil fraction toward the interface (33.19% and 34.06%), as obtained results are shown in Fig. 3.

The presence of CTAB and sulfate anions (SO_4^{2-}) in the brine results in a highly stable emulsion, different from those formed in divalent cation-enriched systems. The key mechanism involves a synergistic interaction, where sulfate ions promote the accumulation of cationic surfactant CTAB at the oil-water interface[2,40,58]. This dense surfactant layer considerably enhances the electrostatic repulsive forces between droplets.

This surfactant-dominated mechanism results in a notable decrease in solid content within the emulsion (5%). The repulsive forces between the negatively charged sulfate ions and the polar asphaltene components limit the opportunity for direct asphaltene-ion or resin-ion complexes and subsequent aggregation. Consequently, the system shows reduced entrapment of asphaltenic or resinc solids compared to emulsions formed with Mg^{2+} or Ca^{2+}, where such complexation is prevalent.

A comparison between (SW10d.2SO4) and (SW10d.4SO4) reveals the role of ionic strength. High sulfate concentrations enhance the salting-out effect rather than the salting-in effect, which reduces the accumulation of CTAB at the interface and compresses the electrical double layer. The resultant strong electrostatic barrier is the primary factor hindering droplet coalescence, leading to enhanced emulsion stability as reflected in Fig. 3. The net effect of this process is dual-fold: it generates a stable emulsion while simultaneously minimizing the incorporation of asphaltenes and resins. According to Fig. 3, this shift away from asphaltene-mediated

stabilization is highly advantageous, leading to a noticeably greater recovery of free oil—approximately 39.88% in the case of (SW10d.4SO4). Thus, sulfate-enriched brines enhance oil recovery more effectively than cation-dominated brines, which tend to cause aggregation and form problematic emulsions. Following the emulsion stability measurements, a series of laboratory tests was performed to probe the mechanisms governing oil-water-rock interactions. The results of these investigations are detailed in the subsequent sections.

Fluid-fluid interactions

Interfacial tension (IFT)

The behavior of oil-water systems is profoundly influenced by interfacial tension (IFT), a key parameter in enhanced oil recovery (EOR) and emulsion stability studies[64,65]. Accurate measurement of interfacial tension (IFT) provides critical insight into the properties of the oil-water interface, which can be altered by several factors. These include the ionic profile of the injected brine, the natural surfactant content of the crude oil (e.g., asphaltenes and resins), and the introduction of synthetic surfactants such as cetyltrimethylammonium bromide (CTAB)[30,66]. In particular, the application of low-salinity water flooding, a common EOR technique, relies on modifying interfacial properties to improve oil displacement[40]. A potentially significant yet less explored aspect is the synergistic effect between brine ions and cationic surfactants like CTAB, which may lead to substantial interfacial tension (IFT) reduction. To investigate these interactions, the interfacial tension (IFT) between the crude oil and various aqueous solutions was measured, and the results are presented in Fig. 4.

Figure 4. demonstrates the strong influence of ionic composition on the interfacial tension (IFT) of crude oil in the brines in the presence of CTAB and calcite particles. Among all tested brines, sulfate-enriched seawater ($SW10d.4SO_4$) produced the lowest interfacial tension (IFT) values, whereas magnesium-rich brines (SW10d.2Mg and SW10d.4Mg) resulted in the highest interfacial tension (IFT). The interfacial tension (IFT) performance follows this order: sulfate-rich brines ($SW10d.4SO_4$: 5.5 mN/m; $SW10d.2SO_4$: 6.9 mN/m) > SW10d (11.1 mN/m) > calcium-rich brines (SW10d.2Ca: 14.8 mN/m; SW10d.4Ca: 16.2 mN/m) > standard seawater (18.3 mN/m) > magnesium-rich brines (SW10d.2Mg: 20.6 mN/m; SW10d.4Mg: 22 mN/m). This hierarchy arises from the combined effects of change in electrical double layer thickness, CTAB accumulation, and asphaltene interactions with solid particles and ions at the oil–water interface.

The interfacial tension (IFT) trend aligns closely with the emulsion stability results (Figs. 2 and 3). The lowest interfacial tension (IFT) in sulfate-rich systems corresponds to the slowest emulsion separation and the highest oil fraction in the emulsion, whereas the high interfacial tension (IFT) observed in magnesium-rich brines coincides with rapid emulsion separation and higher solid content. This association demonstrates that brine composition influences interfacial tension and, in turn, governs emulsion stability as well as the distribution of oil and solid phases.

In sulfate-rich systems, SO_4^{2-} ions play a dual role. First, they increased the negative charge of the interface, which promoted stronger electrostatic attraction for the cationic head groups of CTAB molecules. This increased surfactant accumulation promotes the formation of a dense interfacial film, which effectively lowers

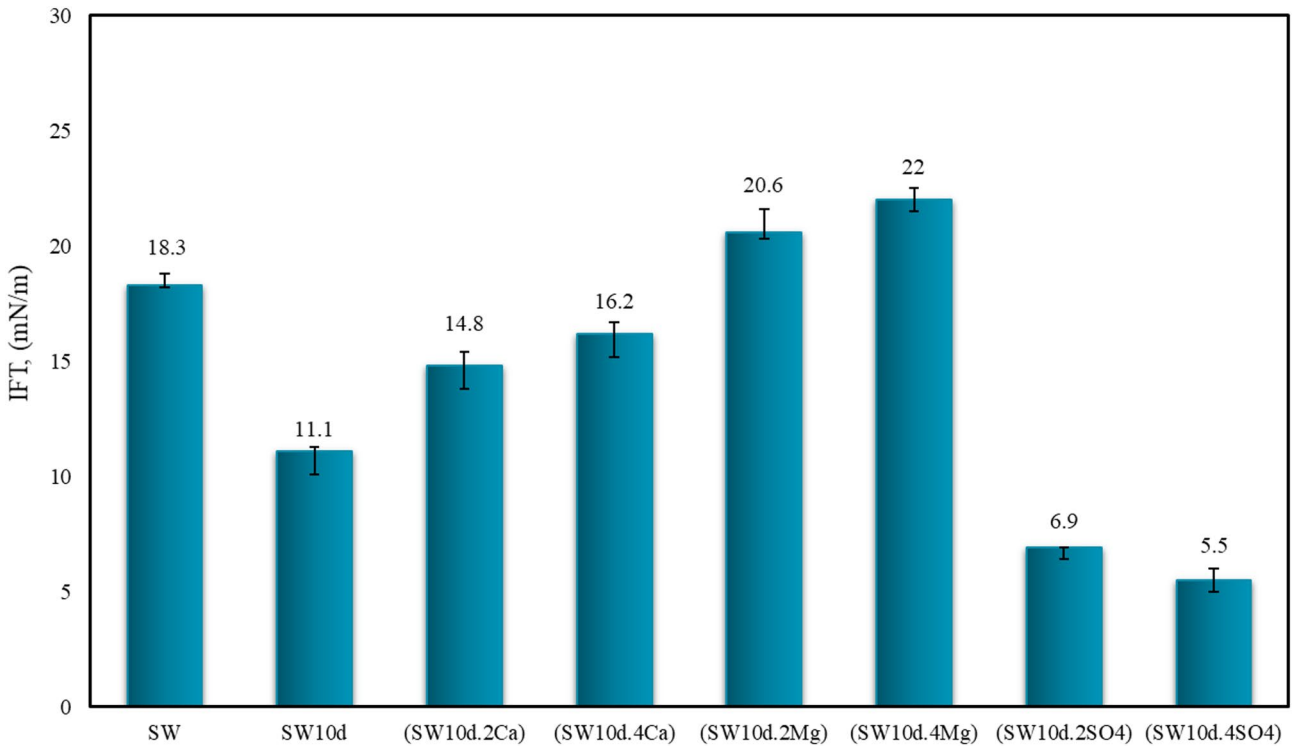

Fig. 4. Interfacial tension (IFT) values between crude oil and different aqueous phases.

the interfacial tension[2,37]. Second, sulfate anions repel negatively charged polar components of crude oil, such as asphaltenes and resins, limiting their ability to accumulate at the interface and form rigid asphaltene-ion or resin-ion complexes. As a result, the oil–($SW10d.4SO_4$) system displayed the sharpest reduction in interfacial tension (IFT), 17 mN/m lower than its magnesium-rich samples. The strong electrostatic repulsion at the CTAB-dominated interface explains the observed high stability and larger oil fraction of emulsions in $SW10d.4SO_4$ (Figs. 2 and 3). This highlights the role of surfactant-coated droplet interactions in stabilizing the interface and facilitating oil mobilization.

By contrast, magnesium-rich brines showed much weaker interfacial tension (IFT) reduction. Magnesium's small ionic radius and high charge density make it a particularly strong competitor for interfacial sites, displacing CTAB molecules and hindering their adsorption. Additionally, Mg^{2+} ions interact with negatively charged groups on asphaltenes (e.g., carboxylates and sulfoxides), forming dense asphaltene–ion layers at the interface[2,17,60]. These rigid films limit CTAB activity and accumulation at the interface, resulting in higher interfacial tension values of 20.6 mN/m for SW10d.2Mg and 22 mN/m for SW10d.4Mg, as illustrated in Fig. 4. Hence, magnesium enrichment both inhibits CTAB from reducing the interfacial tension and promotes rigid asphaltene films, conditions that are generally unfavorable for enhanced oil recovery, as discussed in Sect. 3.1.

Calcium-rich systems (SW10d.2Ca and SW10d.4Ca) exhibited intermediate behavior. Although Ca^{2+} can also form complexes with asphaltenes, its larger ionic radius and lower charge density compared to Mg^{2+} make it less competitive with CTAB. Consequently, CTAB molecules maintained a stronger presence at the calcium-enriched seawater–oil interface, as reflected by the measured interfacial tension (IFT) values of 14.8 mN/m (SW10d.2Ca) and 16.2 mN/m (SW10d.4Ca).

A concentration-dependent effect was also observed: lower Ca^{2+} concentration (SW10d.2Ca) facilitates CTAB adsorption by expanding the electrical double layer and reducing ionic competition. Nevertheless, higher Ca^{2+} concentration (SW10d.4Ca) compresses the electrical double layer, partially restricting CTAB accumulation and resulting in a slightly higher interfacial tension (IFT). Compared with magnesium-containing systems, calcium-rich brines are therefore more effective in reducing interfacial tension (IFT) and enhancing oil recovery. These findings are consistent with the emulsion stability results, where calcium-rich brines exhibited moderate stability and solid content, intermediate between the extremes observed for sulfate-rich and magnesium-rich systems.

The role of ionic strength is further highlighted in the comparison between standard SW and SW10d. In seawater, high ionic strength compressed the EDL and activated the salting-out effect, which inhibited CTAB accumulation and favored the formation of rigid asphaltene–ion complexes. Consequently, the interfacial tension (IFT) remained relatively high at 18.3 mN/m. However, SW10d reduced ionic strength, expanded the EDL, and decreased competition from divalent cations. This facilitated greater migration of CTAB molecules to the interface, lowering the interfacial tension (IFT) to 11.1 mN/m. The comparison between SW and SW10d demonstrated that reducing cation concentration enhanced the effectiveness of CTAB, even in the absence of sulfate enrichment.

Oil zeta potential

To better understand the effect of polar and negative component migration on oil properties, the zeta potential of the aged oil samples was investigated. The observed changes are reported in Fig. 5.

The crude oil sample exhibited a zeta potential of approximately − 30 mV; however, when the oil was exposed to different brines, the zeta potential of the aged oils shifted toward less negative values, ranging from − 16.7 to

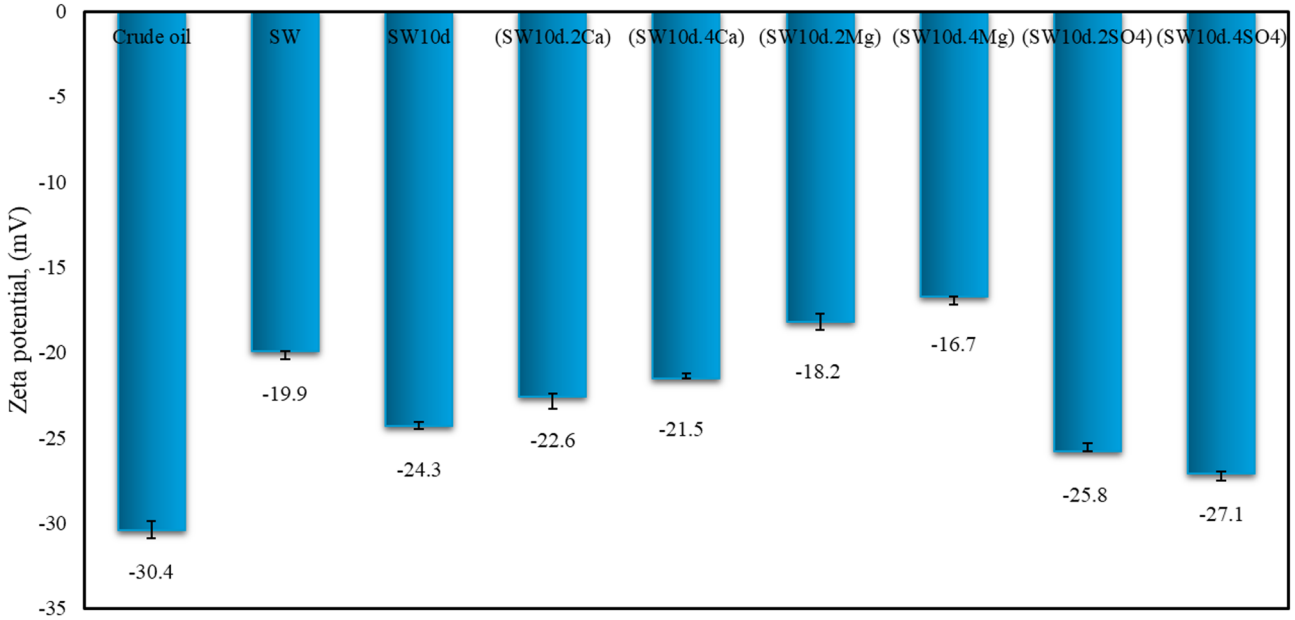

Fig. 5. The result of zeta potential measurements of different aged oils.

−27.1 mV. This change shows that the oil phases lost part of their surface charge when ions, CTAB, or calcite were present. A weaker negative charge means the natural repulsion between oil droplets was reduced, which makes the oil more sensitive to the type of ions in the brine.

The change in surface charge is mainly caused by the migration of asphaltene and resin molecules[15,63]. Asphaltenes and resins are large surface-active molecules that contain oxygen, sulfur, and nitrogen groups[38,67]. These polar groups carry negative charges and tend to accumulate at the oil–water interface. When divalent cations such as Mg^{2+} and Ca^{2+} are present, they interact with these polar sites[17]. The ions neutralize the negative charges and form complexes, which adsorb asphaltenes and resins from the oil bulk and into the interface. This reduces the amount of polar material left in the oil and shifts the zeta potential toward less negative values. The more strongly the ions bind with asphaltene and resin molecules, the greater the reduction in charge.

Among all systems, the magnesium-rich brine exhibited the most pronounced effect. Mg^{2+}, with its small ionic radius and high charge density, effectively forms complexes with asphaltenes and resins at the oil–water interface. As a result, the zeta potential shifted to −16.7 mV, as can be seen in Fig. 5. These molecular-level interactions are directly reflected in the macroscopic behavior: the interfacial tension (IFT) increased sharply in magnesium-rich brines (Fig. 4), and the emulsions separated rapidly (Fig. 2), indicating weak electrostatic repulsion and low emulsion stability. In addition, the extensive migration of asphaltenes from the oil bulk reduced the concentration of polar and negative functional groups in the oil phase, contributing to the high solid fraction observed in Fig. 3 for (SW10d.4Mg).

Calcium-enriched seawater led to a reduction in the oil surface charge, but the effect was weaker than that observed for magnesium-enriched seawater, as shown in Fig. 5. The zeta potential in the calcium-rich system was measured at −21.5 mV. The intermediate value suggests that calcium ions promote negatively charged asphaltene migration from oil bulk compared to sulfate-encrusted seawater and SW10d, although their formation of asphaltene–ion complexes is weaker than that of magnesium ions because of their lower charge density. Correspondingly, the interfacial tension (IFT) for calcium-rich brines was intermediate (14.8–16.2 mN/m), and the emulsions separated more slowly than in magnesium systems but faster than in sulfate-rich systems.

On the other hand, oil exposed to sulfate-enriched seawater in the presence of calcite and CTAB behaved oppositely. Being negatively charged, sulfate did not form strong complexes with asphaltene and resin molecules. Instead, it expanded the electrical double layer around the droplets and helped preserve a more negative surface charge. The zeta potential of the sulfate-rich sample was −27.1 mV, very close to the crude oil value.

This preservation of negative charge correlates with the lowest interfacial tension (IFT) observed for oil in ($SW10d.4SO_4$) (5.5 mN/m, Fig. 4) and with the slowest emulsion separation (Fig. 2). This highlights that electrostatic repulsion between droplets plays a key role in emulsion stability. More asphaltenes remained in the oil bulk rather than migrating to the interface. With more polar components in the oil phase, the interfacial tension (IFT) stayed lower compared with Mg^{2+} or Ca^{2+} systems. The stronger negative surface charge enhanced the accumulation of CTAB molecules at the interface and increased electrostatic repulsion between droplets, resulting in more stable emulsions with slower phase separation. This is consistent with the larger oil fraction (~39.88%) observed in the emulsion phase for sulfate-rich brines (Fig. 3).

Additionally, zeta potential measurements revealed a stronger reduction for aged oil–SW compared with aged oil–SW10d. As discussed in Sect. 3.1 and 3.2.2, this difference arises from variations in the EDL. In the diluted brine (SW10d), the EDL is more expanded, which enhances the accumulation of CTAB molecules at the interface. In contrast, in the case of SW, the higher concentration of active cations increases the affinity of asphaltenes and resins for the interface. This interaction results in partial depletion of negatively charged polar species, such as asphaltenes and resins, from the oil phase. The trend displayed in Fig. 5. provides clear evidence of these effects.

Contribution of the oil components in the emulsion

SARA analysis

The stability of crude oil emulsions is mainly influenced by polar fractions of oil, such as asphaltenes and resins. These polar fractions act like surfactants, which determine the characteristics of the oil-water interface[17]. We conducted the SARA analysis to investigate the individual roles of these components. Figure 6. presents our findings on how resins and asphaltenes distinctly influence emulsion phase behavior.

As can be seen in Fig. 6, the results strongly suggest that asphaltenes are the more dominant fraction compared to resins in governing the oil's properties, especially in response to changes in salinity and ion type.

The most important observation is that the amount of asphaltenes and resins changed in opposite ways when different ions were added. Specifically, when the concentration of calcium (Ca^{2+}) and magnesium (Mg^{2+}) ions increased, the amount of asphaltenes decreased. For example, with more magnesium (aged oil-SW10d.4Mg), asphaltenes in aged oil samples dropped from 12.11% to 9.79%. This happens because these ions help asphaltenes clump together and fall out of the oil. Resins also decrease slightly, but the change is much smaller. This shows that the environment had a stronger and more direct impact on asphaltenes and resins, which were more stable in the oil phase.

On the other hand, when sulfate (SO_4^{2-}) ions were added, the opposite occurred. The amount of asphaltenes increased, from 12.11% to 13.57%. Resins also increased a small amount. This likely happened because sulfate ions made the asphaltene molecules more stable and able to stay dissolved in the oil bulk. Again, the change in the asphaltene percentage was much larger than the change in resins, proving they are more reactive and less stable in the oil phase compared to resin molecules.

Furthermore, a more significant reduction in the asphaltene content was observed in the aged oil-SW, compared to the aged oil-SW10d. This indicates that the specific composition of the water phase plays a critical role in determining which components migrate out of the oil. The reason for this difference lies in the competition for space at the oil-water interface. The SW10d solution contains a higher concentration of the

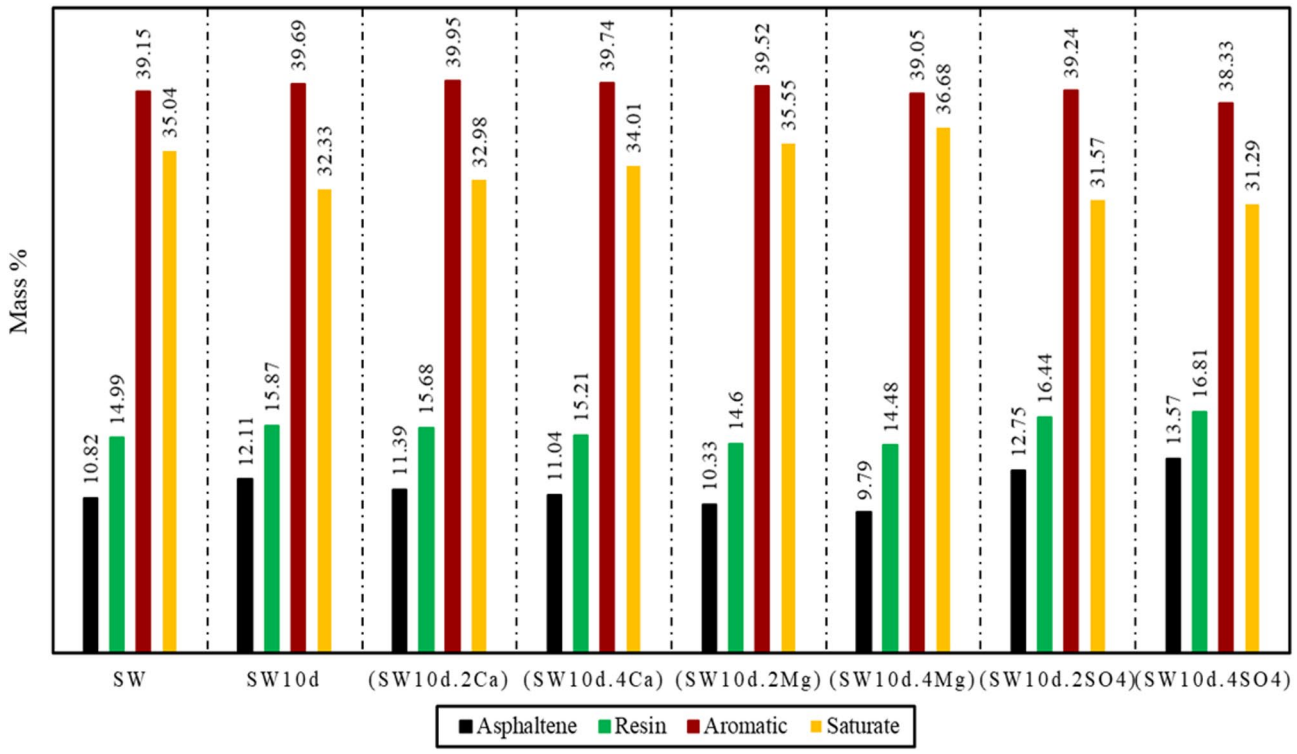

Fig. 6. SARA fractionation results for aged oils.

CTAB molecule. These CTAB molecules effectively dominate the interface, forming a barrier that prevents the migration of asphaltenes from oil toward the interface.

In contrast, SW had fewer CTAB molecules as a result of a greater presence of active cations in the emulsion phase. Without this competition, a larger number of asphaltene molecules were able to migrate and accumulate at the interface. In both samples, the resin molecules showed minimal change, remaining dissolved in the oil phase because they are less surface-active.

This behavior is ultimately due to the innate properties of the molecules. Although asphaltenes are large, they contain polar sections (nitrogen, sulfur, and oxygen, or NSO compounds) that improve the affinity of asphaltene molecules to the interface rather than the oil phase. It can be concluded that asphaltenes are the dominant fraction in changes of oil properties and interfacial phenomena. They are less stable and more reactive to changes in the water chemistry than resins[17,58,68]. Their behavior dictates what happens to the entire oil mixture. Understanding this dominance is key to predicting problems like emulsion stability and designing better processes to break them.

The integrated SARA analysis provided conclusive validation that asphaltenes are the predominant fraction in emulsion stability. This was evidenced by the reduction of asphaltene concentration of the oil phase, while resin concentrations remained largely unchanged. To better clarify how the molecular structure of asphaltene molecules affects oil properties, FTIR analysis was conducted in the following section.

Fourier-transform infrared (FTIR)

The stability of oil–water emulsions during smart water flooding is strongly influenced by the type and distribution of functional groups in crude oil. High-polar components, such as asphaltenes, migrate to the oil–water interface, while less-polar hydrocarbons have less tendency to move toward the interface[10,16,17]. FTIR spectroscopy is particularly useful for monitoring these structural changes, as it allows direct identification of both highly polar and less polar functional groups[17,44]. In this study, FTIR was applied to crude and aged oil samples (Fig. 7), with the outcomes summarized in Table 4 and the quantitative indices listed in Table 5.

As can be observed in Fig. 7, the normalized FTIR spectra revealed five consistent absorption bands across all samples. No additional peaks appeared and none disappeared, meaning that aging under different brine conditions did not generate new functional groups. Instead, the intensity of existing peaks changed, reflecting variations in concentration. This observation is in agreement with previous work on heavy oils[44,69], where the main chemical structure was preserved during aging, but redistribution of aliphatic and aromatic structures was detected.

As shown in Table 4, crude oil spectra featured distinct absorption in the 2720–2735 cm^{-1} region, attributed to C–H stretching in carboxylic acids (HC = O), and a strong band at 2955–2975 cm^{-1} corresponding to CH_3 asymmetric stretching. The band at 1440–1485 cm^{-1} indicated CH_3 bending vibrations, a characteristic signal of aliphatic hydrocarbons, while peaks between 710 and 890 cm^{-1} and the band at 3060 cm^{-1} confirmed the

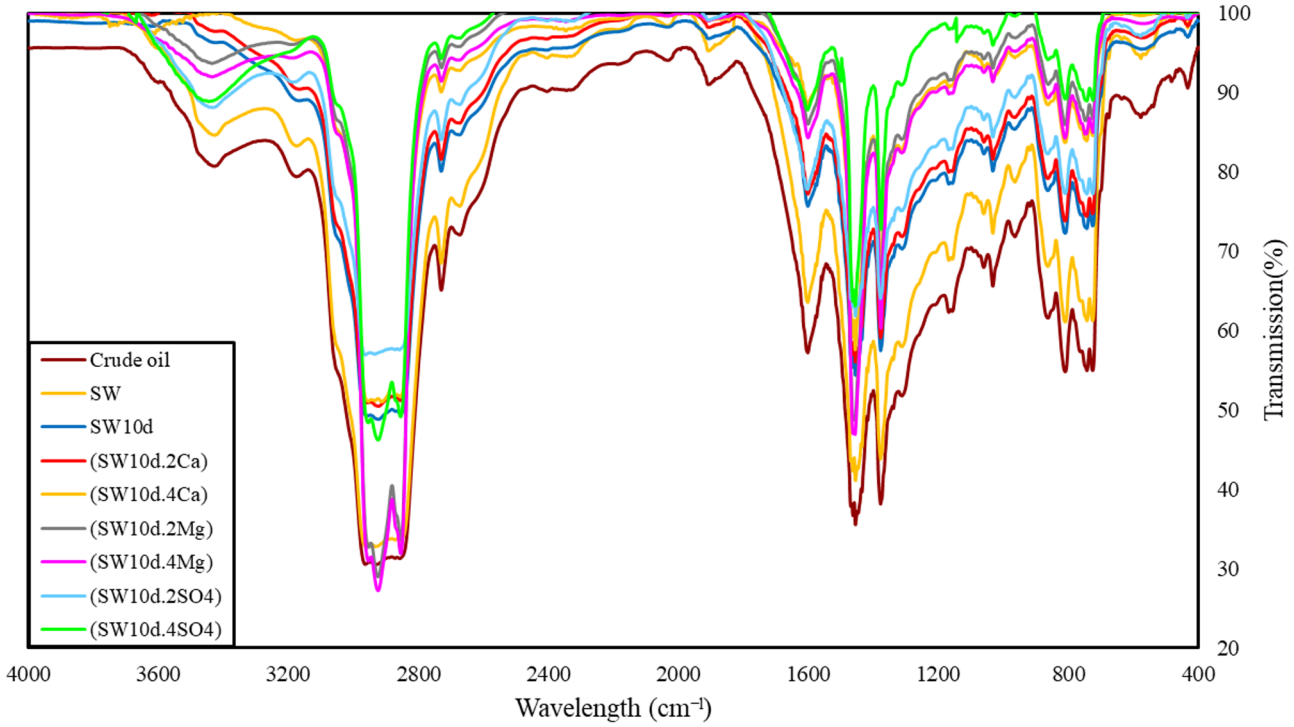

Fig. 7. FTIR spectra of crude and aged oil samples, identifying key functional groups and structural changes.

	Oil
Wavelength(cm^{-1})	Functional groups
3300–3450	O–H stretch (carboxylic acid or Alcohol)
3000–3100	C–H stretch in aromatic
2955–2975	CH3 asymmetric
2910–2940	CH2 symmetric (Alkane)
2800–2860	CH2 asymmetric stretch (Alkane)
2720–2735	HC = O (carboxylic acid)
1904–1910	overtones, weak(aromatic)
1580–1630	C = C stretch (in-ring) aromatic
1440–1485	C–H bend or scissoring
1330–1385	C–H rock, methyl (Alkane)
1150–1200	C–O stretch (Alcohol or Esters or carboxylic acid)
1000–1050	C–O stretch (Alcohol or Esters)
850–890	C–H "oop" (Aromatic)
780–820	C-H (aromatic)
710–760	C–H rock, methyl, seen only in long chain alkanes

Table 4. Assignment of major functional groups and chemical bonds identified in the FTIR spectra of the oil samples[10].

presence of aromatics. Notably, aged oils exhibited reduced intensity in the aliphatic stretching bands (2800–2975 cm^{-1}), consistent with their heavy crude nature, whereas aromatic bands showed relatively stable intensity[70,71]. This contrast illustrates that aliphatic components are more easily mobilized during aging compared to aromatic compounds[44,70].

The functional groups present in the FTIR spectra were quantified by calculating the integral area (A) of the characteristic peaks. These area values were then used to compute several quantitative indices, defined in Eq. 4 through 7, to enable a comparative analysis of the chemical composition across the different oil samples[37,44].

$$ALI\,(Aliphatic\ Index) = \frac{A_{1460} + A_{1376}}{A_{1600} + A_{1460} + A_{1376} + A_{1030} + A_{864} + A_{814} + A_{724} + A_{743} + A_{2953} + A_{2923} + A_{2862}} \quad (4)$$

No	Solutions	ALI	As = o	PA	ARO	LCI
1	Crude oil	0.443	0.780	0.918	0.588	0.402
2	Aged oil-SW	0.241	0.547	0.450	0.375	0.345
6	Aged oil-SW10d	0.292	0.649	0.586	0.455	0.293
3	Aged oil-(SW10d.2Ca)	0.284	0.602	0.539	0.432	0.306
4	Aged oil-(SW10d.4Ca)	0.261	0.579	0.473	0.414	0.324
5	Aged oil-(SW10d.2Mg)	0.227	0.519	0.398	0.329	0.354
7	Aged oil-(SW10d.4Mg)	0.193	0.481	0.366	0.304	0.366
8	Aged oil-(SW10d.2SO4)	0.309	0.656	0.629	0.468	0.263
9	Aged oil-(SW10d.4SO4)	0.331	0.677	0.693	0.484	0.232

Table 5. Quantitative structural indices derived from FTIR analysis.

$$LCI\ (Long\ Chain\ Index) = \frac{A_{724}}{A_{1460} + A_{1376}} \tag{5}$$

$$Polar\ aromatic\ (PA)\ index = \frac{A_{3100-3450}}{A_{1500-1650}} \tag{6}$$

$$ARO\ (\text{Aromaticity})\ index = \frac{A_{1600}}{A_{743} + A_{724} + A_{814}} \tag{7}$$

The derived indices serve as crucial quantitative metrics, allowing for a more robust comparative analysis of the chemical changes evident in the FTIR spectra of the aged oils versus the original crude oil.

In Table 5, the Aliphatic Index (ALI) of crude oil was 0.443 but declined in all aged oils, reaching the lowest value of 0.193 in aged oil-(SW10d.4Mg). This indicates noticeable depletion of aliphatic chains in magnesium-enriched systems. Calcium showed an intermediate effect (0.261 in aged oil-(SW10d.4Ca), while sulfate-rich brines retained more aliphatic fractions (0.331 in aged oil-(SW10d.4SO_4). The decrease in the $A_{S=O}$ index followed the same order (SO_4^{2-}> Ca^{2+} > Mg^{2+}), highlighting the role of sulfoxide-polarized aliphatic branches in promoting interfacial migration. This agrees with earlier reports[45], where sulfoxide groups enhanced the migration of asphaltenes by polarizing attached alkyl chains.

The trends in the ALI and $A_{S=O}$ indices are consistent with the ζ-potential and interfacial tension (IFT) measurements. In magnesium-rich brines, the ζ-potential shifted to − 16.7 mV and the interfacial tension (IFT) reached the highest values (20–22 mN/m). This behavior was attributed to the limited contribution of CTAB at the oil–(SW10d.4Mg) interface, which was insufficient to reduce interfacial tension (IFT). Instead, the migration of polar and negatively charged asphaltenes increased. This is because their sulfoxide-containing aliphatic groups interact with interfacial ions through the complexation mechanism. As a result, asphaltene molecules accumulated at the interface and were depleted from the oil bulk.

These molecular changes are reflected in the emulsion behavior. Figure 3 represents that the least stable emulsion, with a higher solid fraction and a lower oil fraction, was obtained for emulsion-(SW10d.4Mg). Consequently, the emulsion behaved as an asphaltenic emulsion, and the recovery of trapped oil was reduced, as supported by the obtained results from Figs. 2 and 3.

The Long Chain Index (LCI), which measures the contribution of extended alkanes, started at 0.401 in crude oil but declined most sharply in sulfate systems, reaching 0.232 in aged oil-(SW10d.4SO_4). By contrast, oils aged in magnesium-rich brines retained higher values (0.366 in aged oil-(SW10d.4Mg). This shows that sulfate ions predominantly mobilize long-chain hydrocarbons, while magnesium targets polar structures. Similar reductions in aliphatic signals in sulfate-containing systems have been described in prior studies[17,44,72], which SO_4^{2-} was shown to enhance surfactant efficiency and promote micelle formation, facilitating alkane removal from the bulk oil phase.

The Polar Aromatic (PA) and Aromatic Ring (ARO) indices exhibited different patterns. In crude oil, PA and ARO were 0.918 and 0.586, respectively. Oils aged in divalent cation brines showed strong declines: for example, aged oil-(SW10d.4Mg) had PA = 0.365 and ARO = 0.303, while aged oil-(SW10d.4Ca) gave PA = 0.472 and ARO = 0.414. This drop indicates that divalent cations bind to negatively charged asphaltenes, pulling them out of the oil phase and toward the interface. By contrast, sulfate-enriched brines preserved higher values (PA = 0.629–0.693, ARO = 0.468–0.484). Since SO_4^{2-} has no direct affinity for asphaltenes, aromatic fractions largely remained in the oil bulk. Instead, sulfate influenced surfactant behavior indirectly, promoting the mobilization of aliphatic chains rather than aromatics.

When comparing the indices across all oil samples (Table 5), crude oil consistently showed the highest values for ALI (0.443), PA (0.918), and ARO (0.588), indicating its rich content of both aliphatic and aromatic groups before exposure to brines. Once aged, these values declined, but the rate and extent of reduction differed with brine type.

For example, oils aged in magnesium-rich systems displayed the lowest ALI (0.193) and $A_{S=O}$ (0.481), signifying strong depletion of aliphatic fractions and sulfoxide-associated groups. In contrast, sulfate-rich oils retained relatively higher ALI (0.331 in SW10d.4SO_4) and higher PA/ARO values (0.693 and 0.484, respectively), showing that aromatics were preserved while long-chain alkanes were reduced. Calcium-aged oils fell between

these extremes (ALI = 0.260, PA = 0.473, ARO = 0.414), highlighting a moderate effect on both aliphatic and aromatic fractions. Aged oil-SW and aged oil-SW10d also showed reductions, but less pronounced compared with cation- or sulfate-enriched samples, confirming that ion composition has a greater influence than simple dilution.

Direct comparison of the brine systems illustrates these differences more clearly. Sulfate-enriched brines ($SW10d.2SO_4$, $SW10d.4SO_4$) mainly affected the less-polar fractions, lowering the LCI from 0.401 in crude oil to 0.232. At the same time, PA and ARO values stayed high, showing that most aromatics were retained. The ζ-potential results further support these molecular-level observations. In the aged oil-(SW10d.2SO4) and aged oil-(SW10d.4SO4) system, the oil retained more polar aromatic and aliphatic compounds and maintained a more negative ζ-potential (–27.1 mV). The stronger negative charge enhanced the accumulation of CTAB at the oil–water interface, resulting in lower interfacial tension and the formation of the most stable emulsions.

Magnesium-enriched brines (SW10d.2Mg and SW10d.4Mg) resulted significant depletion of asphaltenes containing high concentrations of polar aliphatic and aromatic groups from the oil phase as a result of complexation mechanisms. This was observed by the obtained results of PA, ALI, and aromatic indices in Table 5. Thus, it creates rigid asphaltene-ion complexes at the interface. These complexes reduce the overall negative surface charge of the aged oil, as reflected in the less negative ζ-potential (–16.7 mV), and hinder CTAB accumulation at the interface, leading to higher interfacial tension (20–22 mN/m). Consequently, the emulsions produced in these systems are less stable and separate quickly, as the weakened electrostatic repulsion between droplets facilitates coalescence.

Calcium-enriched systems (SW10d.2Ca, SW10d.4Ca) caused moderate decreases in ALI and aromatic indices, suggesting that asphaltenes rich in aliphatic and aromatic groups partially migrated from the oil phase to the interface. Ca^{2+} ions form complexes with polar oil molecules but, due to their lower charge density, compete less strongly with CTAB. This allows CTAB to partially dominate the interface, generating moderate interfacial tension (IFT) values (14.8–16.2 mN/m) and more stable emulsions, while the zeta potential shifts moderately (–21.5 mV). The mechanism involves a balance between asphaltene–ion complex formation and surfactant-mediated stabilization, resulting in intermediate emulsion behavior compared to aged oil-(SW10d.2Mg) and aged oil-(SW10d.4Mg).

Base seawater (SW and SW10d) showed only modest decreases in FTIR indices (e.g., ALI = 0.241, PA = 0.450, ARO = 0.375), reflecting weaker interfacial interactions and limited migration of polar and aliphatic components. The ζ-potential remained moderately negative, allowing partial electrostatic stabilization of droplets, while interfacial tension (IFT) values (11.1–18.3 mN/m) indicate intermediate surfactant activity. These molecular-level effects collectively lead to emulsions of moderate stability, with droplet coalescence that was not fully prevented.

Fluid-solid interactions

Zeta (ζ) potential of calcite particles

When calcite particles contact water containing dissolved salts and CTAB, some of their surface groups ionize. This ionization produces electrical charges at the rock–water interface, which then affect how stable the particles are in suspension and how they interact with fluids[15,73]. The strength of these surface charges can be evaluated using zeta potential measurements, a technique often used to understand changes in rock wettability[74,75]. It depends on many factors, such as the type of ions, their concentration, the pH of the solution, and adsorbed polar compounds onto the particle surfaces[40,75]. In this study, the zeta potential values of calcite particles were measured when exposed to smart water combined with CTAB solutions. The results are presented in Fig. 8.

As presented in Fig. 8, ζ potential values of calcite particles in different brines ranged from 31.6 to 49.2 mV, reflecting the strong influence of brine composition on electrostatic interactions, surfactant adsorption, and emulsion behavior. Diluted seawater (SW10d) exhibited the highest ζ potential (49.2 mV), while sulfate-enriched seawater ($SW10d.4SO_4$) showed the lowest (31.6 mV). This change in zeta potential indicates that ions affect the thickness of the electrical double layer (EDL), the adsorption of CTAB molecules on calcite surfaces, and their competition with surfactants at the interface.

In SW10d, the lower ionic strength and reduced divalent cation content triggered a salting-in effect, expanding the EDL and decreasing competition between CTAB and brine cations. This allowed CTAB molecules to accumulate more efficiently at the calcite surface, increasing positive surface charge and strengthening electrostatic repulsion between particles. In contrast, SW had a smaller ζ potential (34.9 mV) due to EDL compression and the salting-out effect, which reduced CTAB adsorption despite the presence of the same ions[2,76]. Hence, diluted brines enhance surface charge, stabilize particles, and shift the system toward a more water-wet state[77–79]. This directly supports the improved emulsion stability and higher oil entrapment observed in SW10d emulsions (Figs. 2 and 3).

Cation-enriched solutions displayed intermediate behavior. In calcium-rich brines (SW10d.4Ca: 41.7 mV), Ca^{2+} ions partially competed with CTAB due to their larger ionic radius and lower charge density, allowing moderate surfactant adsorption. This enhanced accumulation of CTAB in the interface helped reduce solid migration (asphaltene) into the emulsion, promoting a stable emulsion.

Magnesium-rich brines (SW10d.4Mg: 38.3 mV), on the other hand, had stronger ionic competition. Mg^{2+} ions, with their smaller size and higher charge density, more effectively displaced CTAB from the calcite surface, reducing ζ potential and weakening electrostatic stabilization[2,40]. From a wettability perspective, these results indicate that calcium-enriched brines allow partial CTAB adsorption and moderate surface charge enhancement, whereas magnesium-rich brines hinder surfactant access. As a result, magnesium-rich brines slowed the transition toward water-wet conditions.

The observed variations in ζ potential also align closely with the differences in solid particle concentration within the emulsion phase, as discussed in Sect. 3.1. In systems where ζ potential was high, such as SW10d and

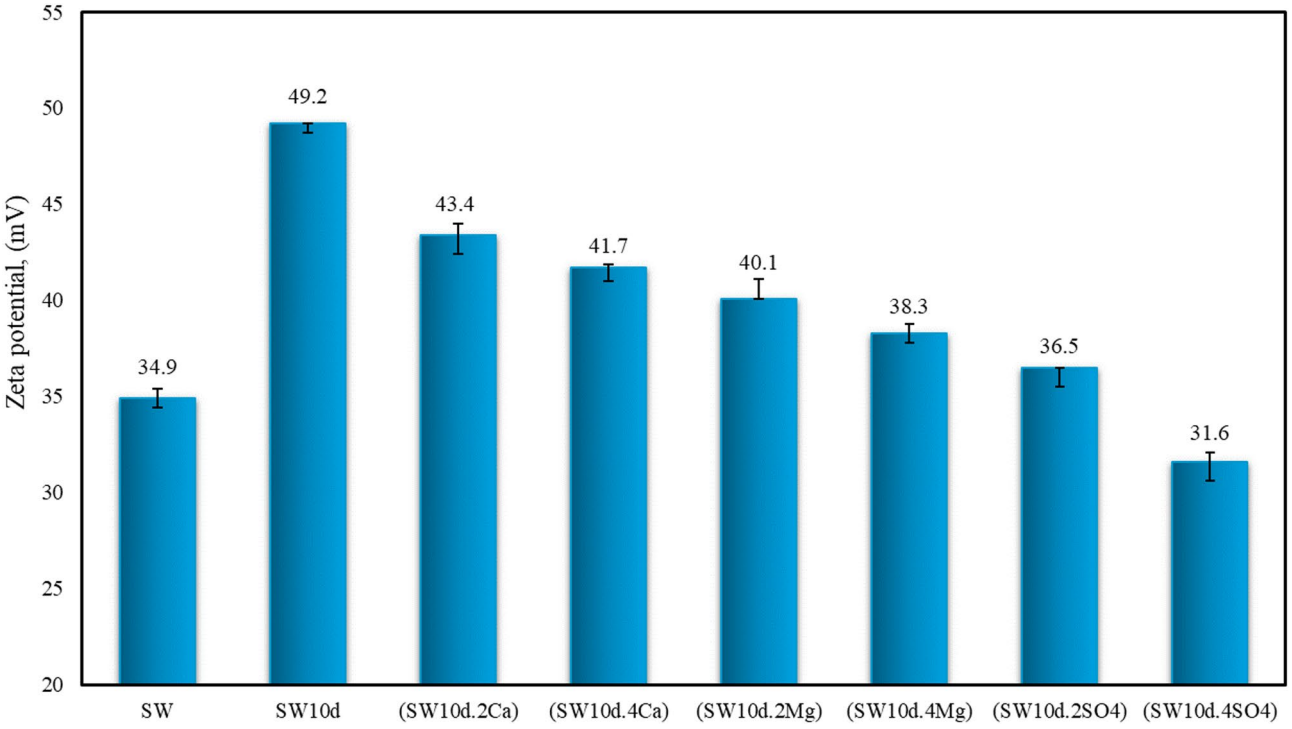

Fig. 8. Zeta potential of dispersed calcite particles in various brine and CTAB solutions.

Ca^{2+}-enriched brines, CTAB adsorption on calcite surfaces was promoted, which stabilized dispersed particles and reduced their migration into the oil phase. This resulted in fewer solid particles being detected in the emulsion, indicating stronger particle–surface attachment and more stable interfacial conditions. Conversely, in Mg^{2+}-enriched systems, the lower ζ potential reflected limited CTAB adsorption due to strong ionic competition; as a result, more calcite particles detached into the emulsion, increasing particle concentration in the oil phase.

Sulfate ions had a distinctive impact on calcite surfaces. In SW10d.2SO_4 (36.5 mV) and SW10d.4SO_4 (31.6 mV), SO_4^{2-} strongly adsorbed onto positively charged calcite, partially inverting the surface charge. At lower sulfate concentrations (SW10d.2SO_4), this allowed partial CTAB neutralization, producing a relatively higher ζ potential. At higher concentrations (SW10d.4SO_4), charge inversion dominated, reducing the ζ potential to its lowest value. Mechanistically, this demonstrates that anion adsorption can both facilitate surfactant alignment at the interface and reduce the net surface charge, thereby modifying particle behavior and interfacial interactions.

From a wettability perspective, sulfate enrichment increases the negative charge on calcite surfaces, which repels negatively charged oil components and enhances water–rock interactions, promoting water-wet conditions.

It should be noted that the measured ζ potential followed the order: SW10d (49.2 mV) > Ca^{2+}-enriched brines (43.4–41.7 mV) > Mg^{2+}-enriched brines (40.1–38.3 mV) > SW (34.9 mV) > SO_4^{2-}-enriched brines (36.5–31.6 mV). These trends are closely related to emulsion stability and wettability alteration: higher ζ potentials correspond to stronger CTAB adsorption, improved particle stabilization, and enhanced water-wet conditions, while lower ζ potentials indicate ionic competition or charge inversion, leading to reduced stabilization and increased solid detachment.

Contact angle

To investigate the combined influence of low salinity water and CTAB molecules on wettability modification, the rock's contact angle was analyzed across multiple solutions. These measurements aimed to assess the interplay between surface interactions at the rock interface and their role in modifying wettability. For reliability, each test was repeated 3 times to confirm results consistency. the averaged contact angles can be seen in Fig. 9.

The contact angle results (Fig. 9) revealed clear differences in wettability depending on the brine composition. Magnesium-enriched systems gave the highest contact angles, with (SW10d.4Mg) reaching 44.5° and (SW10d.2Mg) at 43°, confirming a strongly oil-wet state. By contrast, sulfate-enriched systems displayed the lowest values, with (SW10d.4SO_4) at 32° and (SW10d.2SO_4) at 33.5°, while diluted seawater (SW10d) also gave a relatively low angle of 36°. SW sample showed a higher angle than these diluted or sulfate systems but remained below the Mg-rich cases, while calcium-enriched samples fell between the extremes, with (SW10d.4Ca) at 40° and (SW10d.2Ca) at 38.5°. These data confirm that brine composition controls the extent of wettability alteration, with Mg^{2+} preserving oil-wetness and SO_4^{2-} promoting strong water-wetness.

In SW10d, the ζ potential reached its highest value (49.2 mV), showing strong electrostatic repulsion and stable particle–surface attachment. This condition promoted CTAB adsorption on calcite and limited asphaltene deposition, which reduced the release of calcite particles into the emulsion. The resulting interfacial stability was

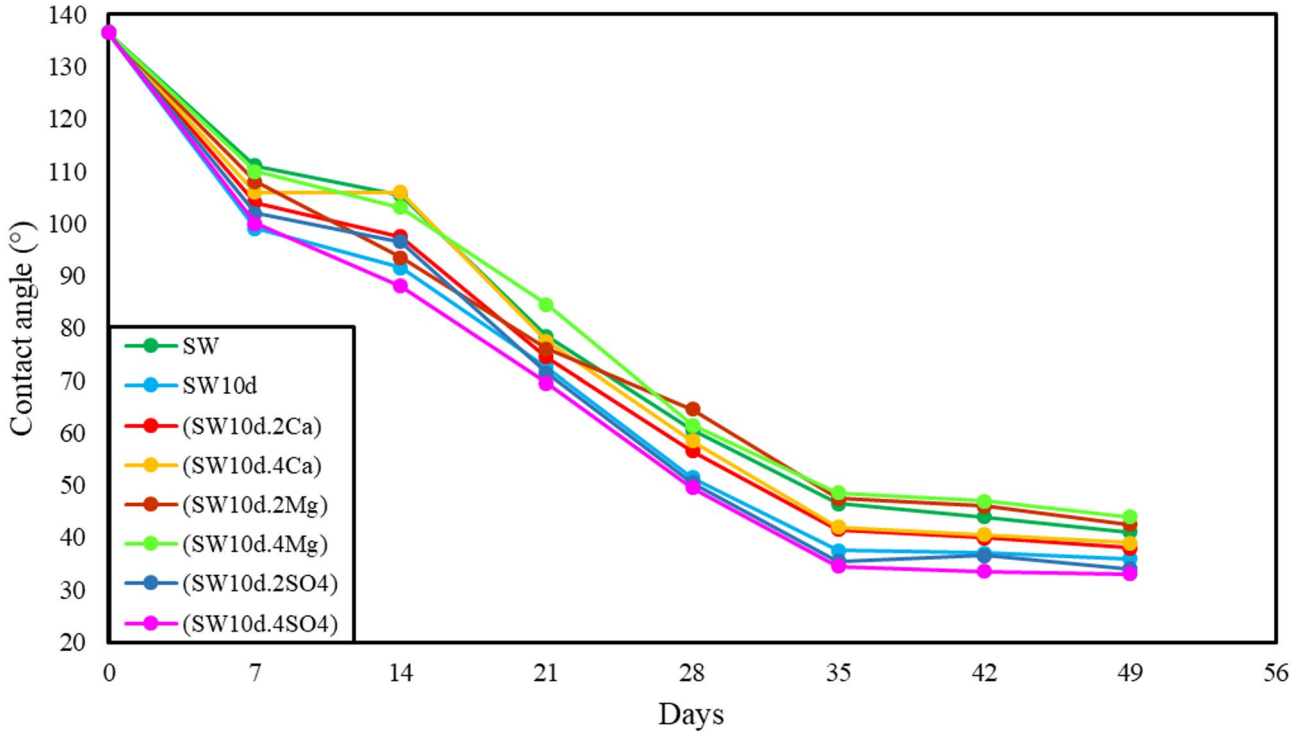

Fig. 9. Contact angle measurements on calcite surfaces after exposure to different ion-surfactant solutions.

reflected in the relatively small contact angle (37° in Fig. 9), indicating enhanced water-wetness compared to SW (34.9 mV, contact angle slightly higher).

However, magnesium-rich systems produced lower ζ potentials (38.3–40.1 mV), where strong ionic competition between Mg^{2+} and CTAB limited surfactant adsorption. At the same time, Mg^{2+}'s high charge density enabled cationic bridging with negatively charged asphaltenes, which destabilized the calcite surface. This promoted particle detachment into the emulsion and resulted in the largest contact angles, up to 44.5° in Fig. 9. These values confirm that Mg^{2+} resists wettability alteration and favors oil-wet states.

Calcium behaved more moderately. Although Ca^{2+} compressed the EDL and competed with CTAB, its larger hydrated radius and lower charge density caused less disruption than Mg^{2+}. Zeta potentials remained relatively higher (41.7–43.4 mV), allowing CTAB to adsorb more effectively and displace Ca^{2+}–asphaltene complexes. This stabilized particle attachment and limited migration into emulsions. The result was intermediate contact angles (38–39° in Figs. 9 and 10), reflecting a partial shift toward water-wetness.

Sulfate systems introduced a different mechanism. Their ζ potentials dropped to the lowest values (31.6–36.5 mV) due to charge inversion caused by SO_4^{2-} adsorption. This created negatively charged calcite surfaces that repelled polar asphaltenes, weakening their attachment. At the same time, SO_4^{2-} did not directly compete with CTAB, enabling the surfactant to adsorb efficiently and form a hydrophilic interfacial layer. As a result, sulfate brines showed the lowest contact angles (32–33.5° in Figs. 9 and 10), representing the strongest water-wet conditions among all brines. The schematic illustrating the wettability alteration and surface charge changes for each sample is shown in Fig. 10.

As shown in Fig. 10, when the synergistic (Mg^{2+} + CTAB) sample was used, the calcite surface became partially water-wet, primarily due to magnesium occupying the surface rather than the accumulation of CTAB molecules. Conversely, the (Ca^{2+} + CTAB) and (SO_4^{2-} + CTAB) showed a higher accumulation of CTAB molecules on the surface compared to (Mg^{2+} + CTAB), particularly in the (SO_4^{2-} + CTAB) sample.

In the (SO_4^{2-} + CTAB) sample, the simultaneous presence of sulfate ions and CTAB molecules on the calcite surface not only reduced the zeta potential but also enhanced the accumulation of CTAB. The negative charge of the sulfate ions facilitated this increased CTAB accumulation, resulting in a more pronounced change in the contact angle. This observation aligns well with the contact angle measurements shown in Fig. 9.

When calcium was used (Ca^{2+} + CTAB), there was less competition between Ca^{2+} ions and CTAB molecules for adsorption sites, allowing more CTAB molecules to attach to the surface. This led to a greater reduction in the contact angle compared to the (Mg^{2+} + CTAB) sample.

The FTIR results (Table 5) further support these observations. The ALI of crude oil was 0.443, but it declined across all aged oils, with the lowest value in Mg-rich systems (0.193 in SW10d.4Mg). This depletion of aliphatic chains corresponds to the low ζ potentials and high contact angles seen in Fig. 9, confirming magnesium's strong impact on polar aliphatic groups. Calcium produced intermediate ALI values (0.259 in SW10d.4Ca), consistent with its moderate ζ potentials and intermediate contact angles. Sulfate systems retained higher ALI (0.330 in SW10d.4SO_4) but exhibited the sharpest decline in the Long Chain Index (LCI, from 0.402 in crude oil

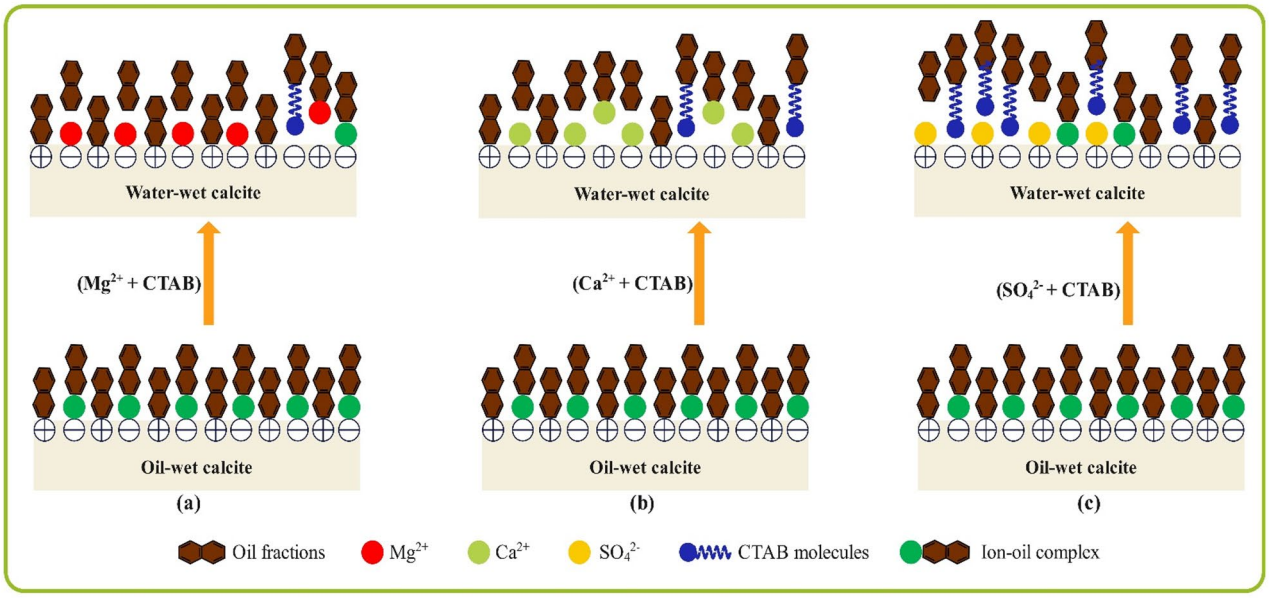

Fig. 10. Schematic illustration of wettability alteration of the calcite surface via the synergistic effect of (**a**) (Mg^{2+} + CTAB), (**b**) (Ca^{2+} + CTAB), and (**c**) (SO_4^{2-} + CTAB).

to 0.232). This suggests sulfate preferentially mobilizes long-chain hydrocarbons while leaving aromatic groups more intact, as indicated by relatively high PA (0.629–0.693) and ARO (0.469–0.483) values. These preserved aromatic fractions explain why sulfate systems maintained strong CTAB performance and the lowest contact angles (33–34° in Fig. 9).

SW and SW10d samples showed moderate reductions in FTIR indices compared with ion-enriched systems. For instance, aged oil in SW retained ALI = 0.241, PA = 0.450, and ARO = 0.375. The higher ζ potential of calcite particles in SW10d (49.2 mV) promoted CTAB adsorption, limited particle detachment into emulsions, and reduced the contact angle to 36° (Fig. 9) compared with standard SW. These results indicate that dilution primarily modifies electrostatic conditions and reduces cation competition, improving wettability without inducing the extensive compositional changes observed in ion-enriched brines.

Conclusions

This research introduced a novel methodology for managing the challenging emulsions formed during low salinity water flooding in carbonate reservoirs. The key finding is that combining sulfate-rich brines with the cationic surfactant CTAB creates the synergy for enhancing oil recovery. This combination produces stable emulsions, lowers interfacial tension, maintains favorable surface charges, and improves wettability, outperforming brines enriched with magnesium or calcium. The supporting evidence from various analyses is as follows:

(1) Sulfate-rich brines produced the most stable emulsions, trapping the highest volume of oil. On the other hand, magnesium-enriched brines promoted rapid formation of rigid asphaltene complexes. This caused fast separation and high solid content, which improved formation damage.
(2) The simultaneous presence of sulfate ions and CTAB resulted in the lowest interfacial tension (IFT) values. This enabled CTAB to dominate the interface and form flexible films that facilitate oil droplet mobility. In contrast, magnesium and calcium ions competed with CTAB, promoting the formation of rigid asphaltene films. This led to the highest interfacial tension (IFT) and hindered oil displacement.
(3) Zeta potential analysis of the aged oils showed that magnesium and calcium ions reduced negatively charged asphaltene molecules in the oil phase, neutralizing the oil's surface charge. This reduction in electrostatic repulsion made emulsions less stable. Sulfate-rich brines, however, helped the oil retain its natural negative charge, leading to stronger repulsive forces between droplets and more stable emulsion systems that are beneficial for oil recovery.
(4) SARA analysis showed that asphaltenes were the main fraction of the oil involved in emulsion interactions, contributing more than other components, especially resins.
(5) FTIR analysis showed that various functional groups contributed to the interfacial interactions and phenomena. In magnesium-rich brines, polar asphaltenes were strongly depleted from the oil bulk (ALI = 0.193, PA = 0.365, ARO = 0.303), confirming their role in forming rigid solid complexes at the interface. In contrast, sulfate-enriched brines preserved a higher fraction of polar asphaltenes (PA = 0.693, ARO = 0.484) while selectively mobilizing less-polar asphaltenes (LCI = 0.232), supporting enhanced surfactant activity, lower interfacial tension (IFT), and more stable emulsions.

(6) High positive zeta potentials and low contact angles in sulfate and diluted brines confirmed the effective accumulation of CTAB on calcite, rendering the surface strongly water-wet. However, magnesium-rich brines maintained oil-wet conditions, which explains their poor oil recovery performance.

Data availability

All data generated or analyzed during this study are included in this manuscript.

Received: 12 September 2025; Accepted: 4 November 2025
Published online: 09 December 2025

References

1. Al-Shalabi, E. W. & Sepehrnoori, K. A comprehensive review of low salinity/engineered water injections and their applications in sandstone and carbonate rocks. *J. Petrol. Sci. Eng.* **139**, 137–161 (2016).
2. Tajikmansori, A., Dehaghani, A. H. S. & Haghighi, M. Improving chemical composition of smart water by investigating performance of active cations for injection in carbonate reservoirs: A mechanistic study. *J. Mol. Liq.* **348**, 118043 (2022).
3. Lashkarbolooki, M., Riazi, M., Hajibagheri, F. & Ayatollahi, S. Low salinity injection into asphaltenic-carbonate oil reservoir, mechanistical study. *J. Mol. Liq.* **216**, 377–386 (2016).
4. Derkani, M. H. et al. Low salinity waterflooding in carbonate reservoirs: review of interfacial mechanisms. *Colloids Interfaces*. **2** (2), 20 (2018).
5. Balavi, A., Ayatollahi, S. & Mahani, H. The simultaneous effect of Brine salinity and dispersed carbonate particles on asphaltene and emulsion stability. *Energy Fuels*. **37** (8), 5827–5840 (2023).
6. Maghsoudian, A., Izadpanahi, A., Bahmani, Z., Avvali, A. H. & Esfandiarian, A. Utilizing deterministic smart tools to predict recovery factor performance of smart water injection in carbonate reservoirs. *Sci. Rep.* **15** (1), 537 (2025).
7. Shahsavani, B., Riazi, M. & Malayeri, M. R. Asphaltene instability in the presence of emulsified aqueous phase. *Fuel* **305**, 121528, (2021).
8. Zolfaghari, R., Fakhru'l-Razi, A., Abdullah, L. C., Elnashaie, S. S. & Pendashteh, A. Demulsification techniques of water-in-oil and oil-in-water emulsions in petroleum industry. *Sep. Purif. Technol.* **170**, 377–407 (2016).
9. Ghasemian, J., Riahi, S., Ayatollahi, S. & Mokhtari, R. Effect of salinity and ion type on formation damage due to inorganic scale deposition and introducing optimum salinity. *J. Petrol. Sci. Eng.* **177**, 270–281 (2019).
10. Mahdavi, M. S., Tajikmansori, A., Saeedi Dehaghani, A. H. & Seyed Mousavi, S. A. H. The synergic effect of Brine salinity and dispersed clay particles on Water-in-Heavy oil emulsion: insight into asphaltene structure and emulsion stability. *SPE J.* 1–17, (2024).
11. Ma, J., Yao, M., Yang, Y. & Zhang, X. Comprehensive review on stability and demulsification of unconventional heavy oil-water emulsions. *J. Mol. Liq.* **350**, 118510 (2022).
12. Pickering, S. U. Cxcvi.—emulsions. *J. Chem. Soc. Trans.* **91**, 2001–2021 (1907).
13. Wang, Z., Babadagli, T. & Maeda, N. Generation of Pickering emulsions by activating natural asphaltenes as nano materials: an experimental analysis for cost-effective heavy-oil recovery. *J. Mol. Liq.* **339**, 116759 (2021).
14. Bonto, M., Eftekhari, A. A. & Nick, H. M. An overview of the oil-brine interfacial behavior and a new surface complexation model. *Sci. Rep.* **9** (1), 6072 (2019).
15. Mahdavi, M. S. & Dehaghani, A. H. S. Experimental study on the simultaneous effect of smart water and clay particles on the stability of asphaltene molecule and emulsion phase. *Sci. Rep.* **15** (1), 3393 (2025).
16. Karami, S. & Dehaghani, A. H. S. A molecular insight into cracking of the asphaltene hydrocarbons by using microwave radiation in the presence of the nanoparticles acting as catalyst. *J. Mol. Liq.* **364**, 120026 (2022).
17. Tajikmansori, A., Dehaghani, A. H. S., Sadeghnejad, S. & Haghighi, M. New insights into effect of the electrostatic properties on the interfacial behavior of asphaltene and resin: an experimental study of molecular structure. *J. Mol. Liq.* **377**, 121526 (2023).
18. Liang, C., Liu, X., Jiang, H., Xu, Y. & Jia, Y. Dissipative particle Dynamics-Based simulation of the effect of asphaltene structure on Oil–Water interface properties. *ACS Omega*. **8** (36), 33083–33097 (2023).
19. Joonaki, E., Buckman, J., Burgass, R. & Tohidi, B. Water versus asphaltenes; liquid–liquid and solid–liquid molecular interactions unravel the mechanisms behind an improved oil recovery methodology. *Sci. Rep.* **9** (1), 11369 (2019).
20. Cai, X. et al. Assembling kaolinite nanotube at water/oil interface for enhancing Pickering emulsion stability. *Appl. Clay Sci.* **172**, 115–122 (2019).
21. Zhou, Q. et al. Synergistic effects of Asphaltenes, Kaolinite, and water chemistry on Oil-Water emulsion stability. *Separation Purif. Technol.* 133461, (2025).
22. Seng, L. Y., Al-Shaikh, M. & Hascakir, B. Intermolecular interaction between heavy crude oils and surfactants during surfactant-steam flooding process. *ACS Omega*. **5** (42), 27383–27392 (2020).
23. Dehaghani, A. H. S., Hosseini, M., Tajikmansori, A. & Moradi, H. A mechanistic investigation of the effect of ion-tuned water injection in the presence of cationic surfactant in carbonate rocks: an experimental study. *J. Mol. Liq.* **304**, 112781 (2020).
24. Hou, B. et al. Mechanism of synergistically changing wettability of an oil-wet sandstone surface by a novel nanoactive fluid. *Energy Fuels*. **34** (6), 6871–6878 (2020).
25. Salehi, N., Dehaghani, A. S. & Haghighi, M. Investigation of fluid-fluid interaction between surfactant-ion-tuned water and crude oil: A new insight into asphaltene behavior in the emulsion interface. *J. Mol. Liq.* **376**, 121311 (2023).
26. Maurya, N. K. & Mandal, A. Investigation of synergistic effect of nanoparticle and surfactant in macro emulsion based EOR application in oil reservoirs. *Chem. Eng. Res. Des.* **132**, 370–384 (2018).
27. Jia, H. et al. Mechanism studies on the application of the mixed cationic/anionic surfactant systems to enhance oil recovery. *Fuel* **258**, 116156, (2019).
28. Kamal, M. S., Hussein, I. A. & Sultan, A. S. Review on surfactant flooding: phase behavior, retention, IFT, and field applications. *Energy Fuels*. **31** (8), 7701–7720 (2017).
29. Nourani, M., Tichelkamp, T., Gaweł, B. & Øye, G. Desorption of crude oil components from silica and aluminosilicate surfaces upon exposure to aqueous low salinity and surfactant solutions, *Fuel* **180**, 1–8, (2016).
30. Koreh, P., Lashkarbolooki, M., Peyravi, M. & Jahanshahi, M. Interfacial performance of cationic, anionic and non-ionic surfactants; effect of different characteristics of crude oil. *J. Petrol. Sci. Eng.* **218**, 110960 (2022).
31. Javadi, A. H. & Fatemi, M. Impact of salinity on fluid/fluid and rock/fluid interactions in enhanced oil recovery by hybrid low salinity water and surfactant flooding from fractured porous media. *Fuel* **329**, 125426, (2022).
32. Zallaghi, M. & Khaz'ali, A. R. Experimental and modeling study of enhanced oil recovery from carbonate reservoirs with smart water and surfactant injection. *Fuel* **304**, 121516, (2021).
33. Rezvani, H., Binks, B. P. & Nguyen, D. Surfactant-nanoparticle formulations for enhanced oil recovery in calcite-rich rocks. *Langmuir* **40** (47), 24989–25002, (2024).
34. Liu, Q. et al. Improved oil recovery by adsorption–desorption in chemical flooding. *J. Petrol. Sci. Eng.* **43**, 1–2 (2004).

35. Divandari, H., Hemmati-Sarapardeh, A., Schaffie, M. & Ranjbar, M. Integrating functionalized magnetite nanoparticles with low salinity water and surfactant solution: Interfacial tension study. *Fuel* **281**, 118641, (2020).
36. Li, B. et al. Assessing nanoparticle-surfactant-salt synergistic effects on droplet–droplet electrocoalescence by molecular dynamics simulations. *J. Mol. Liq.* **367**, 120570 (2022).
37. Mahdavi, M. S., Mansouri, A. T. & Dehaghani, A. H. S. Experimental investigation of CTAB modified clay on oil recovery and emulsion behavior in low salinity water flooding. *Sci. Rep.* **15** (1), 21471 (2025).
38. Taherian, Z., Dehaghani, A. S., Ayatollahi, S. & Kharrat, R. The mechanistic investigation on the effect of the crude oil/brine interaction on the interface properties: A study on asphaltene structure. *J. Mol. Liq.* **360**, 119495 (2022).
39. Yang, F. et al. Pickering emulsions stabilized solely by layered double hydroxides particles: the effect of salt on emulsion formation and stability. *J. Colloid Interface Sci.* **302** (1), 159–169 (2006).
40. Tajikmansori, A., Hosseini, M. & Dehaghani, A. H. S. Mechanistic study to investigate the injection of surfactant assisted smart water in carbonate rocks for enhanced oil recovery: an experimental approach. *J. Mol. Liq.* **325**, 114648 (2021).
41. Naser, M. A., Permadi, A. K., Bae, W., Ryoo, W. & Siregar, S. A laboratory investigation of the effects of saturated steam properties on the interfacial tension of heavy-oil/steam system using pendant drop method. *Energy Environ. Res.* **5** (1), 94 (2015).
42. Drelich, J., Fang, C. & White, C. Measurement of interfacial tension in fluid-fluid systems. *Encyclopedia Surf. Colloid Sci.* **3**, 3158–3163 (2002).
43. Mehraban, M. F., Farzaneh, S. A., Sohrabi, M. & Sisson, A. Fluid-fluid interactions inducing additional oil recovery during low salinity water injection in inefficacious presence of clay minerals. *Fuel* **308**, 121922, (2022).
44. Zojaji, I., Esfandiarian, A. & Taheri-Shakib, J. Toward molecular characterization of asphaltene from different origins under different conditions by means of FT-IR spectroscopy. *Adv. Colloid Interface Sci.* **289**, 102314 (2021).
45. Karami, S., Dehaghani, A. S. & Haghighi, M. Analytical investigation of asphaltene cracking due to microwave and ultrasonic radiations: A molecular insight into asphaltene characterization and rheology. *Geoenergy Sci. Eng.* **233**, 212481 (2024).
46. Wang, B., Ma, S., Li, Y. P., Wang, N. & Ren, Q. X. Axial compression mechanical properties of UHTCC–hollow steel tube square composited short columns. *J. Constr. Steel Res.* **228**, 109424 (2025).
47. Wang, B., Zhao, S., Ren, Q. X. & Xie, R. Q. Axial compressive behavior of circular Hollow steel tube-reinforced UHTCC column. *Structures* **71**, 107943. (2025).
48. Austad, T., RezaeiDoust, A. & Puntervold, T. Chemical mechanism of low salinity water flooding in sandstone reservoirs. In *SPE Improved Oil Recovery Conference?* pp. SPE-129767-MS. (Spe, 2010).
49. Zhang, P., Tweheyo, M. T. & Austad, T. Wettability alteration and improved oil recovery by spontaneous imbibition of seawater into chalk: impact of the potential determining ions Ca2+, Mg2+, and SO42–. *Colloids Surf., A.* **301**, 1–3 (2007).
50. Wang, B. et al. Study of bond-slip push-out test of circular Hollow steel tube and UHTCC. *J. Constr. Steel Res.* **223**, 109043 (2024).
51. Ren, Q. X., Zhou, K. & Li, W. Experimental study of clay concrete filled steel tubular stub columns under axial compression. *Structures* **70**, 107509. (2024).
52. Taheri-Shakib, J., Shekarifard, A. & Naderi, H. Inhibiting asphaltene precipitation using microwave irradiation: experimental investigation. In *Saint Petersburg 2018*, vol. 2018, no. 1, 1–5. (European Association of Geoscientists & Engineers, 2018).
53. Chakraborty, R. et al. Synergistic effects of nonionic surfactant and organic alkali for enhanced oil recovery: optimizing interfacial tension reduction, emulsion stability, and corrosion control under optimal salinity conditions. *Energy Fuels* (2025).
54. Kazemzadeh, Y., Ismail, I., Rezvani, H., Sharifi, M. & Riazi, M. Experimental investigation of stability of water in oil emulsions at reservoir conditions: Effect of ion type, ion concentration, and system pressure. *Fuel* **243**, 15–27, (2019).
55. Yekeen, N., Padmanabhan, E., Syed, A. H., Sevoo, T. & Kanesen, K. Synergistic influence of nanoparticles and surfactants on interfacial tension reduction, wettability alteration and stabilization of oil-in-water emulsion. *J. Petrol. Sci. Eng.* **186**, 106779 (2020).
56. Farhadi, H., Ayatollahi, S. & Fatemi, M. The effect of Brine salinity and oil components on dynamic IFT behavior of oil-brine during low salinity water flooding: diffusion coefficient, EDL establishment time, and IFT reduction rate. *J. Petrol. Sci. Eng.* **196**, 107862 (2021).
57. Lyu, C., Zhong, L., Ning, Z., Chen, M. & Cole, D. R. Review on underlying mechanisms of low salinity waterflooding: comparisons between sandstone and carbonate. *Energy Fuels*. **36** (5), 2407–2423 (2022).
58. Lashkarbolooki, M., Riazi, M., Ayatollahi, S. & Hezave, A. Z. Synergy effects of ions, resin, and asphaltene on interfacial tension of acidic crude oil and low–high salinity brines. *Fuel* **165**, 75–85, (2016).
59. Mokhtari, R., Hosseini, A., Fatemi, M., Andersen, S. I. & Ayatollahi, S. Asphaltene destabilization in the presence of an aqueous phase: the effects of salinity, ion type, and contact time. *J. Petrol. Sci. Eng.* **208**, 109757 (2022).
60. Mokhtari, R., Ayatollahi, S. & Fatemi, M. Experimental investigation of the influence of fluid-fluid interactions on oil recovery during low salinity water flooding. *J. Petrol. Sci. Eng.* **182**, 106194 (2019).
61. Moradi, M., Topchiy, E., Lehmann, T. E. & Alvarado, V. Impact of ionic strength on partitioning of naphthenic acids in water–crude oil systems–Determination through high-field NMR spectroscopy. *Fuel* **112**, 236–248, (2013).
62. Banerjee, S., Zhang, Z. Q., Hall, A. S. & Thoi, V. S. Surfactant perturbation of cation interactions at the electrode–electrolyte interface in carbon dioxide reduction. *ACS Catal.* **10** (17), 9907–9914 (2020).
63. Lashkarbolooki, M., Ayatollahi, S. & Riazi, M. Effect of salinity, resin, and asphaltene on the surface properties of acidic crude oil/smart water/rock system. *Energy Fuels*. **28** (11), 6820–6829 (2014).
64. Noorizadeh Bajgirani, S. S. & Saeedi Dehaghani, A. H. Experimental investigation of wettability alteration, IFT reduction, and injection schemes during surfactant/smart water flooding for EOR application. *Sci. Rep.* **13** (1), 11362 (2023).
65. Mansouri Zadeh, M., Amiri, F., Hosseni, S. & Ghamarpoor, R. Synthesis of colloidal silica nanofluid and assessment of its impact on interfacial tension (IFT) and wettability for enhanced oil recovery (EOR). *Sci. Rep.* **14** (1), 325 (2024).
66. Ramezani, M., Lashkarbolooki, M. & Abedini, R. Experimental investigation of different characteristics of crude oil on the interfacial activity of anionic, cationic and nonionic surfactants mixtures. *J. Petrol. Sci. Eng.* **214**, 110485 (2022).
67. Mahdavi, S. & Mousavi Moghadam, A. Critical review of underlying mechanisms of interactions of asphaltenes with oil and aqueous phases in the presence of ions. *Energy Fuels*. **35** (23), 19211–19247 (2021).
68. Lashkarbolooki, M. & Ayatollahi, S. Effect of asphaltene and resin on interfacial tension of acidic crude oil/sulfate aqueous solution: experimental study. *Fluid. Phase. Equilibria*. **414**, 149–155 (2016).
69. Karami, S., Dehaghani, A. H. S. & Mousavi, S. A. H. S. Condensate blockage removal using microwave and ultrasonic waves: discussion on rock mechanical and electrical properties. *J. Petrol. Sci. Eng.* **193**, 107309 (2020).
70. Taheri-Shakib, J., Saadati, N., Esfandiarian, A., Hosseini, S. A. & Rajabi-Kochi, M. Characterizing the wax-asphaltene interaction and surface morphology using analytical spectroscopy and microscopy techniques. *J. Mol. Liq.* **302**, 112506 (2020).
71. Taheri-Shakib, J., Esfandiarian, A., Rajabi-Kochi, M., Kazemzadeh, E. & Afkhami Karaei, M. Evaluation of rock and fluid intermolecular interaction between asphaltene and sand minerals using electrochemical, analytical spectroscopy and microscopy techniques. *Sci. Rep.* **14** (1), 670 (2024).
72. Liu, S. et al. Effect of dispersants on the stability of calcite in non-polar solutions. *Colloids Surf., A*. **672**, 131730 (2023).
73. Boumedjane, M., Karimi, M., Al-Maamari, R. S. & Aoudia, M. Experimental investigation of the concomitant effect of potential determining ions Mg2+/SO42 – and Ca2+/SO42 – on the wettability alteration of oil-wet calcite surfaces. *J. Petrol. Sci. Eng.* **179**, 574–585 (2019).
74. Farhadi, H., Fatemi, M. & Ayatollahi, S. Experimental investigation on the dominating fluid-fluid and rock-fluid interactions during low salinity water flooding in water-wet and oil-wet calcites. *J. Petrol. Sci. Eng.* **204**, 108697 (2021).

75. Taheri-Shakib, J. et al. A comprehensive study of asphaltene fractionation based on adsorption onto calcite, dolomite and sandstone. *J. Petrol. Sci. Eng.* **171**, 863–878 (2018).
76. Paria, S. & Khilar, K. C. A review on experimental studies of surfactant adsorption at the hydrophilic solid–water interface. *Adv. Colloid Interface Sci.* **110** (3), 75–95 (2004).
77. Eriksson, R., Merta, J. & Rosenholm, J. B. The calcite/water interface: I. Surface charge in indifferent electrolyte media and the influence of low-molecular-weight polyelectrolyte. *J. Colloid Interface Sci.* **313** (1), 184–193 (2007).
78. Derkani, M. H. et al. Mechanisms of surface charge modification of carbonates in aqueous electrolyte solutions. *Colloids Interfaces.* **3** (4), 62 (2019).
79. Cicerone, D. S., Regazzoni, A. E. & Blesa, M. A. Electrokinetic properties of the calcite/water interface in the presence of magnesium and organic matter. *J. Colloid Interface Sci.* **154** (2), 423–433 (1992).

Author contributions

A.T.M: Conceptualization, Investigation, Methodology, Formal analysis, Writing, review & editing.M.S.M: Conceptualization, Formal analysis, Investigation, Methodology, Writing. A.H.S.D: Resources, Funding acquisition, Supervision.

Declarations

Competing interests

The authors declare no competing interests.

Additional information

Correspondence and requests for materials should be addressed to A.H.S.D.

Reprints and permissions information is available at www.nature.com/reprints.

Publisher's note Springer Nature remains neutral with regard to jurisdictional claims in published maps and institutional affiliations.